The Plant Cell, Vol. 24: 4670–4686, November 2012, www.plantcell.org

A Galactoglycerolipid Lipase Is Required for Triacylglycerol Accumulation and Survival Following Nitrogen Deprivation in *Chlamydomonas reinhardtii*[C][W]

Xiaobo Li,[a,b] Eric R. Moellering,[a,c,1] Bensheng Liu,[c] Cassandra Johnny,[c] Marie Fedewa,[c] Barbara B. Sears,[b] Min-Hao Kuo,[c] and Christoph Benning[c,2]

[a] Department of Energy–Plant Research Laboratory, Michigan State University, East Lansing, Michigan 48824
[b] Department of Plant Biology, Michigan State University, East Lansing, Michigan 48824
[c] Department of Biochemistry and Molecular Biology, Michigan State University, East Lansing, Michigan 48824

Following N deprivation, microalgae accumulate triacylglycerols (TAGs). To gain mechanistic insights into this phenomenon, we identified mutants with reduced TAG content following N deprivation in the model alga *Chlamydomonas reinhardtii*. In one of the mutants, the disruption of a galactoglycerolipid lipase-encoding gene, designated *PLASTID GALACTOGLYCEROLIPID DEGRADATION1* (*PGD1*), was responsible for the primary phenotype: reduced TAG content, altered TAG composition, and reduced galactoglycerolipid turnover. The recombinant PGD1 protein, which was purified from *Escherichia coli* extracts, hydrolyzed monogalactosyldiacylglycerol into its lyso-lipid derivative. In vivo pulse-chase labeling identified galactoglycerolipid pools as a major source of fatty acids esterified in TAGs following N deprivation. Moreover, the fatty acid flux from plastid lipids to TAG was decreased in the *pgd1* mutant. Apparently, de novo–synthesized fatty acids in *Chlamydomonas reinhardtii* are, at least partially, first incorporated into plastid lipids before they enter TAG synthesis. As a secondary effect, the *pgd1* mutant exhibited a loss of viability following N deprivation, which could be avoided by blocking photosynthetic electron transport. Thus, the *pgd1* mutant provides evidence for an important biological function of TAG synthesis following N deprivation, namely, relieving a detrimental overreduction of the photosynthetic electron transport chain.

INTRODUCTION

Triacylglycerol (TAG) is a universal storage lipid in plants, algae, fungi, and animals. TAG is composed of a glycerol backbone to which three fatty acyl chains are esterified. By transesterification with methanol, TAG can be converted into fatty acid methylesters commonly referred to as biodiesel (Durrett et al., 2008). Microalgae have been considered as a sustainable feedstock for the production of biofuels because they accumulate substantial amounts of TAG following nutrient deprivation. Theoretical calculations suggest that microalgae can surpass crop plants in their TAG yield per land area used (Weyer et al., 2010). Despite the recent interest in microalgae, this phylogenetically diverse group of photosynthetic organisms is not well understood at the molecular and biochemical levels, and the mechanistic basis of algal lipid metabolism and of TAG accumulation still needs to be explored in detail. Much of our current molecular understanding of photosynthetic lipid biosynthesis is based on work with *Arabidopsis thaliana* and other land plant models, providing paradigms that may not be directly transferable given their evolutionary divergence from microalgae. Indeed, our current information on lipid metabolism in the green algal model *Chlamydomonas reinhardtii*, which is mostly based on genome annotation (Riekhof et al., 2005) or early labeling and lipid profiling experiments (Giroud et al., 1988; Giroud and Eichenberger, 1989), suggests that lipid metabolism in this organism is distinct in crucial aspects from that of land plants. Most strikingly, *C. reinhardtii* lacks phosphatidylcholine (PtdCho), but instead contains the betaine lipid diacylglycerol-*N,N,N*,-trimethylhomoserine (DGTS).

Seed plants typically have two assembly pathways for glycerolipids (Roughan and Slack, 1982). Fatty acids are synthesized de novo in the plastid while attached to acyl carrier proteins (ACPs) (Ohlrogge et al., 1979). Acyltransferases at the inner chloroplast envelope membrane transfer acyl groups from acyl-ACPs to glycerol 3-phosphate, leading to the formation of phosphatidic acid, the precursor of glycerolipids of the thylakoid membrane. Alternatively, fatty acids are exported from the plastid for assembly of extraplastidic glycerolipids, including TAGs at the endoplasmic reticulum (ER). Because the acyltransferases associated with the inner plastid envelope membrane and the ER have different acyl group preferences, glycerolipids assembled by the two pathways can be distinguished based on their acyl group composition (Heinz and Roughan, 1983). In *C. reinhardtii*, analysis of the acyl groups in the glyceryl backbone of the galactoglycerolipids, which are the predominant lipids in the thylakoid membranes, suggested that their assembly is completely dependent on the plastid pathway (Giroud et al., 1988). By contrast, in

[1] Current address: Synthetic Genomics, 11149 North Torrey Pines Road, La Jolla, CA 92037.
[2] Address correspondence to benning@msu.edu.
The author responsible for distribution of materials integral to the findings presented in this article in accordance with the policy described in the Instructions for Authors (www.plantcell.org) is: Christoph Benning (benning@msu.edu).
[C] Some figures in this article are displayed in color online but in black and white in the print edition.
[W] Online version contains Web-only data.
www.plantcell.org/cgi/doi/10.1105/tpc.112.105106

seed plants such as *Arabidopsis*, the galactoglycerolipid molecular species are nearly equally derived from the ER and the plastid assembly pathway (Browse et al., 1986), thus requiring an elaborate system of lipid transfer between the ER and the plastid envelopes (Benning, 2009).

In particular, the lack of PtdCho in *C. reinhardtii* is expected to affect other aspects of glycerolipid metabolism. For example, isotope labeling of cytosolic lipids in pea (*Pisum sativum*) leaves indicated that most of the acyl groups synthesized de novo in the plastid are first incorporated into PtdCho instead of phosphatidic acid (Bates et al., 2007). Thus, it was proposed that acyl editing of PtdCho is an important aspect of fatty acid export from the plastid, cycling acyl groups through PtdCho before they enter the cytosolic acyl-CoA pool, which ultimately provides acyl groups for glycerolipid assembly at the ER. The lack of PtdCho in *C. reinhardtii* raises several questions, particularly whether an alternative mechanism of acyl editing, possibly involving DGTS or another lipid, or a mechanism completely independent of acyl editing exists, which is involved in the export of fatty acids from the plastid. These apparent differences in the cellular organization of basic membrane glycerolipid metabolism in *C. reinhardtii* may also extend to differences in the formation of TAGs and their storage in lipid droplets (Liu and Benning, 2012). Typically, lipid droplets are formed at the ER in all eukaryotic cells. However, recent reports on TAG accumulation in *C. reinhardtii* suggest that TAG-containing lipid droplets are present in plastids (Fan et al., 2011; Goodson et al., 2011), raising the possibility that TAG is either directly assembled in plastids or imported into them.

Aside from the basic mechanisms of glycerolipid assembly in *C. reinhardtii*, the details of the regulation of TAG synthesis are unclear as well. Like other microalgae, *C. reinhardtii* produces lipid droplets filled with TAGs following nutrient deprivation (Wang et al., 2009; Moellering and Benning, 2010), conditions that involve genome-wide transcriptional changes (Miller et al., 2010; Castruita et al., 2011). Intriguingly, among the genes upregulated or downregulated by N deprivation were a large number of genes annotated to encode lipases (Miller et al., 2010). One of the downregulated genes was recently shown to encode a lipase involved in TAG turnover in *C. reinhardtii* (Li et al., 2012). As a complement to transcript profiling in revealing genes involved in TAG metabolism or its regulation, we developed a genetic screen for mutants with abnormal TAG levels following N deprivation. Here, we describe the identification of a low-TAG mutant with a lesion in a galactoglycerolipid lipase-encoding gene. This gene was among the upregulated lipase-encoding genes following N deprivation (Miller et al., 2010), consistent with a role for acyl editing or turnover of galactoglycerolipids during TAG formation in *C. reinhardtii*. The availability of a low TAG mutant of *C. reinhardtii* also allowed us to examine the physiological role of TAG accumulation following nutrient stress.

RESULTS

Isolation of TAG Mutants

To generate *C. reinhardtii* mutants with altered TAG content, random, insertional gene disruption was conducted by introducing a linearized pHyg3 plasmid (Berthold et al., 2002) into the cell wall–less *C. reinhardtii* strain dw15-1, which is referred to as the parental wild-type strain (because it is wild-type with regard to its lipid content and synthesis). Hygromycin B-resistant transgenic lines were picked into a 96-well plate and induced for TAG accumulation by transfer to low-N medium. During the primary screen, Nile Red fluorescence staining of neutral lipids (Kimura et al., 2004; Chen et al., 2011) was used to monitor neutral lipids in a high-throughput mode using a 96-well plate reader. Putative mutants differing in Nile Red fluorescence from the wild-type parental strain based on statistical criteria (as defined in Methods) were reanalyzed by extracting lipids and separating them by thin layer chromatography (TLC), followed by quantification of TAG-derived fatty acid methylesters by gas–liquid chromatography. Of 34,000 independent transgenic lines generated, 80 were initially found to exhibit an altered Nile Red fluorescence intensity, of which six mutants with robust and reproducible changes in TAG levels were eventually isolated. The focus here is on the characterization of one of the low-TAG mutants, initially designated line E12. After in-depth analysis it was renamed *plastid galactoglycerolipid degradation1* (*pgd1*), which is the designation used from here on.

The *pgd1* Mutant Has Reduced TAG and Becomes Chlorotic Following N Deprivation

Over the course of 3 d following N deprivation, the *pgd1* mutant showed an ~50% reduction in the ratio of fatty acids in TAG over total fatty acids in the lipid extract, a parameter that allows a robust comparison of relative TAG content between different lines, in this case *pgd1* and the wild-type parental strain dw15-1 (Figure 1A). Because nonhomologous integration of linearized plasmids into the *C. reinhardtii* genome can potentially occur multiple times in a single line, genetic linkage of the hygromycin B resistance and the lipid phenotype were examined to confirm insertional tagging of the gene responsible for the lipid phenotype, a prerequisite for subsequent gene identification. Toward this end, the *pgd1* mutant was crossed with CC-198, a cell-walled strain (mating type$^-$) and close relative of dw15-1, which is mating type$^+$ and the wild-type parental strain of *pgd1*. Strains CC-198 and dw15-1 were compared for their lipid composition but did not show major differences in TAG content. The ratio of fatty acids in TAG over total fatty acids in extracts was 0.46 $\pm$ 0.04 for dw15-1 and 0.51 $\pm$ 0.04 for CC-198. A total of 83 meiotic progeny lines were analyzed, of which 40 were resistant and 43 sensitive to hygromycin B. The observed ratio approached the hypothetical 2:2 segregation ratio, suggesting a single plasmid insertion in the genome, although the statistical limitations of the experiment would allow for multiple, but very tightly linked, plasmid insertions. Lipid analysis was performed on 14 progeny lines (Figure 1B), and the results were compared with the wild-type parental strain and *pgd1*. The TAG fatty acid over total fatty acid ratio of the eight hygromycin B sensitive lines was similar to that of the parental strain, while the six resistant lines showed a ratio similar to that of the original *pgd1* mutant. Thus, the hygromycin B resistance marker appeared to be closely linked to the mutation causing the lipid phenotype.

In addition to TAG deficiency, *pgd1* cells gradually developed chlorosis and fully bleached over the course of 12 d following N

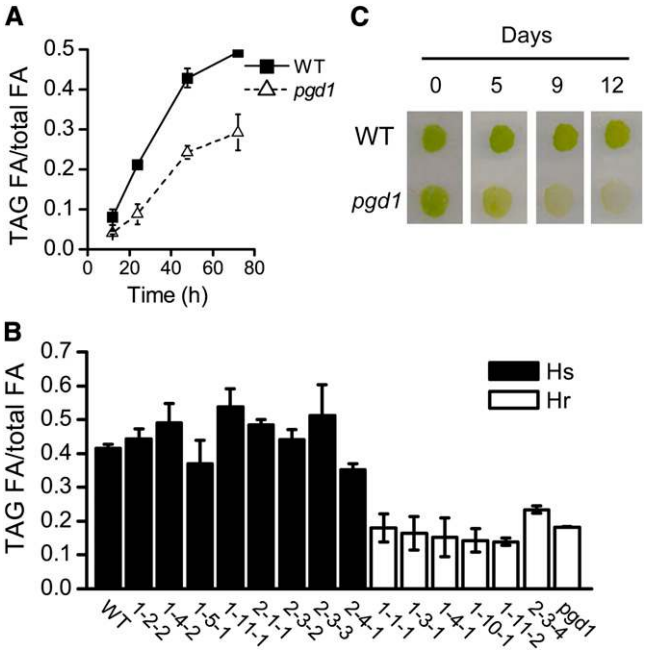

Figure 1. Phenotypes of the *pgd1* Mutant Compared with the Wild-Type Parental Strain.

(A) and **(B)** Time course of TAG accumulation following N deprivation **(A)** and phenotypic analysis of progenies from a cross between *pgd1* and CC-198 **(B)**. Hs and Hr indicate hygromycin B–sensitive and –resistant lines, respectively. The ratio of fatty acids (FA) in TAGs over total fatty acids in the lipid extracts is shown. Averages of three independent measurements are provided. Error bars indicate SD. WT, the wild type.
(C) Appearance of the same patches of N-deprived cells placed on agar-solidified TAP-N medium, 0 to 12 d after plating.

depletion (Figure 1C), which was accompanied by reduced cell viability (see below). However, in N-replete medium, there was no discernible difference in growth between the wild-type parental strain and *pgd1* (see Supplemental Figure 1 online). Thus, the ability to produce or maintain TAG seems to be required for the long-term viability of the cells following N deprivation, which provides a clue toward a physiological role of TAG accumulation under nutrient stress, which will be further explored below.

The *pgd1* Lipid Phenotype Is Caused by Disruption of a Putative Lipase Gene

To identify the plasmid insertion site, SiteFinding PCR (Tan et al. 2005) was employed. Random primers combined with primers annealing to the positive strand of the hygromycin B resistance gene (*aph7″*) on the pHyg3 plasmid (Figure 2A, primer S1) generated two partial pHyg3 plasmid sequences present in opposite orientations, as depicted in Figure 2A, but no bona fide genomic flanking DNA. Probing a DNA gel blot of *Bam*HI-digested *pgd1* genomic DNA with a pHyg3 fragment as indicated in Figure 2A, two signals were observed (Figure 2B), although only one would be expected for a single insertion due to the presence of a single *Bam*HI site in pHyg3. However, probing *pgd1* genomic DNA double-digested with *Pst*I (no site in pHyg3) and *Xho*I (single site in pHyg3) with the same probe, a single band was present (Figure 2B). Together, these data suggested that two pHyg3 fragments were present in opposite orientations at the *pgd1* locus. No true signal was obtained from genomic DNA of the wild-type parental strain (Figure 2B).

Through SiteFinding PCR with plasmid-specific, nested primers S2-1 and S2-2 complementary to the other end of pHyg3 (Figure 2A, S2), a flanking genomic DNA (to the right side of the insertion as shown in Figure 2A) was amplified. Sequencing indicated that one end of the insertion bordered sequences within the predicted untranslated region of a gene previously annotated as *CGLD15* (for *CONSERVED IN GREEN LINEAGE AND*

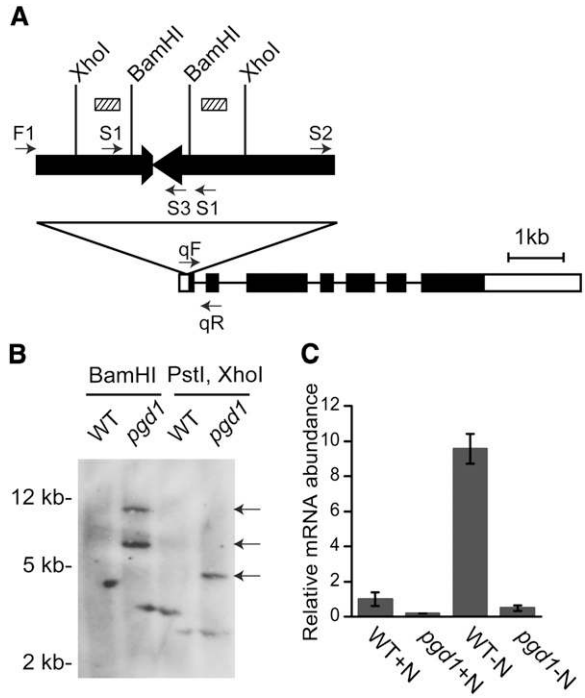

Figure 2. Molecular Characterization the *pgd1* Mutant.

(A) A schematic representation of the pHyg3 insertion into the genome of the *pgd1* mutant. The triangle represents the insert. Thick arrows indicate the orientation of the positive strand of the *aph7″* gene conferring resistance to hygromycin B. The *PGD1* gene model is shown in a 5′ to 3′ direction from left to right, with exons and introns represented by black boxes and connecting lines, respectively. The 5′ and 3′ untranslated regions are shown as white boxes. Crosshatched boxes indicate the position of the DNA gel blot probe used in **(B)**. PCR primer sites are indicated by arrows, which are not drawn to scale. The binding sites for the SiteFinding primers and nested primers for the two ends of the insertion are shown as single arrows S1 and S2, respectively. Sequences for all primers can be found in Supplemental Table 1 online.
(B) DNA gel blot of the pHyg3 insertion and surrounding genomic DNA. Genomic DNA was digested with *Bam*HI or *Pst*I and *Xho*I and probed with the fragment (cross-hatched box) as shown in **(A)**. *Pst*I cuts outside the insert and sites are not shown in **(A)**. WT, the wild type.
(C) Quantitative RT-PCR of the *PGD1* transcript in the wild-type parental strain and the *pgd1* mutant grown for 48 h in TAP (+N) or TAP-N (−N) medium. The abundance of *PGD1* mRNA was normalized to *RACK1*. Data are presented as average ± SD ($n = 3$).

DIATOMS15; Chlamydomonas v5.3 genome in the Phytozome database, http://www.phytozome.net/) on chromosome 3 (position 6320421 to 6327099; gene locus Cre03.g193500) (Merchant et al., 2007), which we designated *PGD1* based on functional analysis presented below. A conserved catalytic triad of Ser-Asp-His was predicted for the translated protein sequence of this gene, which is a typical motif for hydrolases such as lipases (acyl hydrolases). The flanking genomic sequence on the left side of the insertion (refer to Figure 2A) was obtained by PCR with primers F1 and S3 (Figure 2A). Sequence analysis of this fragment showed that the insertion was accompanied by the deletion of 14 bp of genomic sequence that is unlikely to affect the neighboring gene 5′ to *PGD1*. Based on these analyses, *PGD1* was considered the most likely affected gene in the *pgd1* mutant responsible for the observed lipid phenotype.

Insertions into the promoter or untranslated region of *PGD1* were expected to affect gene expression. Quantifying *PGD1* transcript levels by real-time PCR (Figure 2C) showed greatly reduced expression of this gene in the *pgd1* mutant. The real-time PCR results also confirmed the increased expression of *PGD1* in the wild-type parental strain following N deprivation previously observed during global transcript analysis (Miller et al., 2010). The upregulation of *PGD1* expression following N deprivation in parallel with TAG accumulation suggested that the gene product might play a role in TAG biosynthesis.

To independently confirm that the phenotypes of the *pgd1* mutant were indeed caused by the insertion into *PGD1* described above, complementation analysis with a *PGD1*-containing fragment from the BAC clone 5E6 (Grossman et al., 2003) was conducted. The fragment used for transformation contained 2 kb 5′ and 1 kb 3′ of the predicted *PGD1* gene and was devoid of other predicted open reading frames. The pMN24 plasmid (Fernández et al., 1989) containing the *NIT1* gene encoding nitrate reductase was used in a cotransformation experiment for selection on agar plates with nitrate as the N source. (Note, the parental wild-type strain dw15-1 and *pgd1* carry a mutation in the genomic *NIT1* gene.) To screen for DNA fragments rescuing the observed chlorosis phenotype of *pgd1* on N-limited medium, we developed a single-step N deprivation colony color screen method. Agar plates containing 0.5 mM instead of 10 mM nitrate were used for selection allowing colonies to form, which then became N deprived as nitrate was depleted. Under these conditions, *pgd1* mutant colonies turned from green to white within 3 weeks, while colonies of the wild-type parental strain or *pgd1* colonies harboring an introduced wild-type copy of the *PGD1* gene were expected to remain green (Figure 3A). When the *PGD1* genomic fragment was cotransformed with the *NIT1* marker, ~5 to 10% of the colonies remained green. This frequency is at the lower end of the range for previously reported cotransformation efficiencies (Kindle, 1990). Eight colonies scored as green and another eight colonies scored as white were chosen and the phenotype was confirmed by spotting cells onto −N agar plates (Figure 3B). Genotyping was performed on the junction of the plasmid insertion to confirm the presence of the gene disruption typical for the *pgd1* mutant (Figure 3C). Primers F1 and R were expected to give a signal specific for *PGD1* either in the genome or introduced through the fragment, and primers S2-1 and R were expected to give a signal specific for *pgd1*. According to this reasoning, seven of the eight green lines (G1 to G7) and one

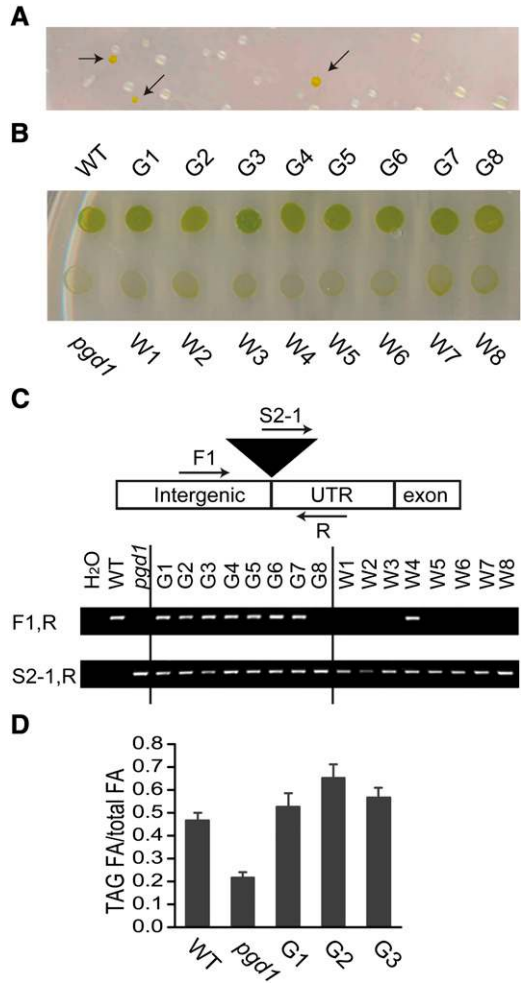

Figure 3. Genetic Complementation of *pgd1* Phenotypes with Wild-Type Genomic DNA.

(A) Section of an agar plate with *pgd1* mutant colonies 20 d after transformation with a wild-type *PGD1*-containing fragment. Green colonies (arrows) are presumed to be complemented lines; white colonies show the chlorosis phenotype characteristic of *pgd1*.

(B) Confirmation of the phenotypes of lines which form green (G1-8) and bleached colonies (W1-8) following restreaking and 10 d of growth on TAP-N. The *pgd1* mutant and the wild-type parental strain (WT) are included.

(C) Genotyping of the different lines. A scheme depicting the insertion site shows the primer locations with arrows; sections of DNA gels with PCR products obtained with PCR primers as indicated are shown below. Primer sizes are not to scale.

(D) Quantitative analysis of TAG of three lines rescued with *PGD1* genomic DNA after 48 h of growth in TAP-N medium. The ratio of fatty acids (FA) in TAGs over total fatty acids in the lipid extracts is shown. Averages of three independent measurements are provided. Error bars indicate SD.

of the white lines (W4) contained the wild-type *PGD1* gene (Figure 3C). The presence of a signal from a combination of S2-1 and R indicative of the presence of the *pgd1* background ruled out contamination by the parental strain. It seems likely that in outlier G8, a secondary mutation caused the observed suppressor

phenotype, and in outlier line W4, the introduced *PGD1* gene was either mutated, not adequately expressed, or silenced. Quantitative lipid analysis of three green colony-forming lines (G1 to G3) showed that they regained their ability to accumulate TAGs to similar levels as the parental strain (Figure 3D).

Extraplastidic Lipids of *pgd1* Are Affected in a Consistent Way

The fact that disrupting *PGD1* led to lower TAG content argues against its gene product's role as a TAG lipase because decreased TAG lipase activity in the mutant would be expected to increase TAG content. An alternative hypothesis was that PGD1 releases acyl groups from membrane lipids. The activation of the released fatty acids by formation of acyl-CoAs would then make them available for TAG synthesis. To identify the lipid substrates for such a presumed lipase, the abundant membrane lipids DGTS, phosphatidylethanolamine (PtdEtn), monogalactosyldiacylglycerol (MGDG), digalactosyldiacylglycerol (DGDG), phosphatidylglycerol (PtdGro), sulfoquinovosyldiacylglycerol (SQDG), and phosphatidylinositol were analyzed in the wild-type parental strain and *pgd1* grown on N-replete and N-depleted medium for 48 h (Figure 4A). The relative fraction of DGDG increased following N deprivation as recently reported (Fan et al., 2011). However, no statistically significant difference between the relative amounts of the respective membrane lipid classes for the wild-type parental strain and the *pgd1* mutant was observed.

Although relative amounts of membrane lipid classes were not altered under the growth conditions used, it seemed possible that specific molecular species within each lipid class represented by differences in the respective acyl group substituents were altered in the mutant. For example, changes in fatty acid profiles of glycerolipids have been diagnostic in determining whether the ER or plastid pathways of lipid assembly were affected in the respective mutants of *Arabidopsis* (Kunst et al., 1988; Xu et al., 2003). Overall, the decreased TAG content in *pgd1* was reflected by a reduced total amount of fatty acids per cell (Figure 4C), raising the question of whether specific TAG molecular species were missing in *pgd1* consistent with the disruption of one of several hypothetical TAG assembly pathways. Indeed, the total fatty acid profile of *pdg1* was altered. Most prominently the relative fraction of oleate (18:1$^{\Delta 9}$; number of carbons:number of double bonds and position of double bonds from the carboxyl end) was reduced (Figure 4B). Following N deprivation, the wild-type parental strain showed an increase in the relative amount of oleate that was not observed for *pgd1*, but the acyl composition of *pgd1* was indistinguishable from that of the parental strain under N-replete growth conditions (Figure 4B). When the fatty acyl group profile of individual lipids following N deprivation was examined, a decrease in oleate was observed for *pgd1* not only in TAG (Figure 4D) but also in DGTS (see Supplemental Figure 2A online) and PtdEtn (see Supplemental Figure 2B online). The latter two are presumed to be extraplastidic membrane lipids (Giroud et al., 1988; Giroud and Eichenberger, 1989), while the exclusive location of TAG in cytosolic lipid droplets has recently been questioned (Fan et al., 2011; Goodson et al., 2011). Oleate accounts for ~25% of the acyl groups in TAG, but only up to 10% in DGTS or

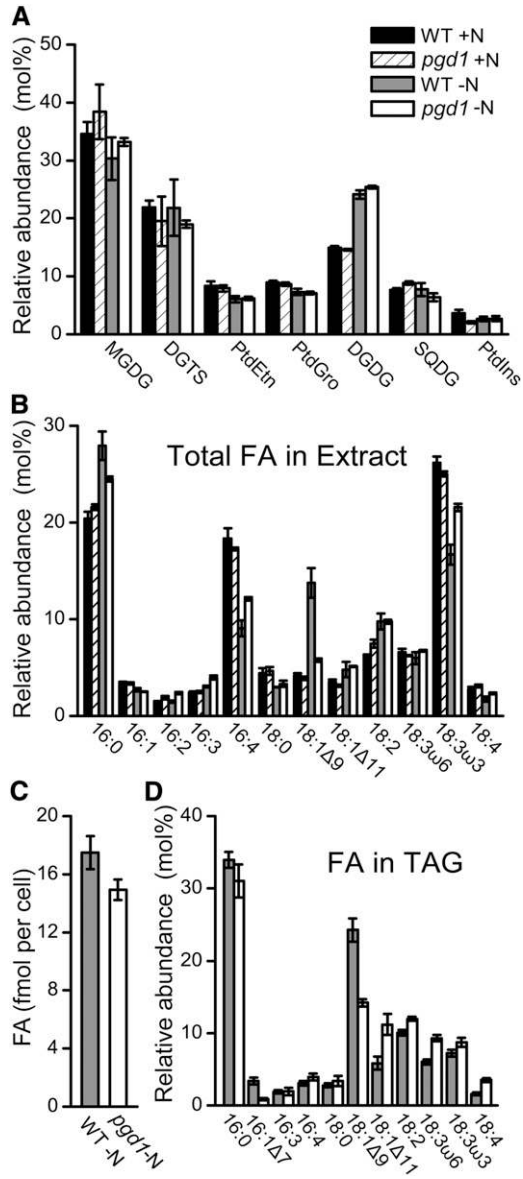

Figure 4. Detailed Lipid Analysis of the Wild-Type Parental Strain and *pgd1* Mutant in N-Replete Medium and 48 h after Transfer to N-Depleted Medium.

(A) Relative abundance of major polar lipid classes.

(B) and **(C)** Relative fatty acid (FA) composition **(B)** and cellular contents of total cellular fatty acids **(C)**.

(D) Composition of fatty acids esterified to TAG. Averages of three replicates are shown with error bars indicating SD.

DGTS, diacylglycerol-*N*, *N*, *N*-trimethylhomoserine; DGDG, digalactosyldiacylglycerol; MGDG, monogalactosyldiacylglycerol; PtdEtn, phosphatidylethanolamine; PtdGro, phosphatidylglycerol; PtdIns, phosphatidylinositol; SQDG, sulfoquinovosyldiacylglycerol. Fatty acids are designated as chain length:number of double bonds. Positions of double bonds are indicated with Δ (counting from carboxyl group) or ω (counting from the methyl group). In **(B)**, 16:2 is a mixture of 16:2 Δ7,10 and 16:2 Δ10,13.

PtdEtn, explaining why a loss of a specific molecular species containing this fatty acid has more drastic effects on overall TAG content than on that of DGTS and PtdEtn. The plastid lipids MGDG (see Supplemental Figure 2C online), DGDG (see Supplemental Figure 2D online), and PtdGro (see Supplemental Figure 2E online) were not altered in their acyl composition. As apparently only extraplastidic lipids are affected in the *pgd1* mutant, it seems possible that PGD1 activity affects the export of acyl groups from the plastid or the assembly of extraplastidic lipids, assuming that the fraction of TAG missing in *pgd1* is extraplastidic.

Oleate Is Decreased in the *sn-1* and *sn-3* Position of TAGs in *pgd1*

To gain more information on the origin of the diacylglycerol moiety for TAG biosynthesis and possible role of oleate ($18:1^{\Delta 9}$) in limiting TAG biosynthesis in *pgd1*, positional analysis of TAG acyl groups was conducted with *Rhizopus arrhizus* lipase. *R. arrhizus* lipase specifically hydrolyzes the *sn-1* position of membrane glycerolipids or the *sn-1*/*sn-3* positions of TAG and is frequently used for the positional analysis of acyl groups in glycerolipids (Fischer et al., 1973; Siebertz and Heinz, 1977). Consistent with previous observations (Fan et al., 2011), the *sn-2* position of TAG is mostly composed of C16 acyl groups but the *sn-1*/*sn-3* positions contain both C16 and C18 acyl groups (Figure 5). A decrease in oleate in the *sn-1* or *sn-3* position was obvious, but the method did not allow us to distinguish between the two positions. For *sn-1*/*sn-3*, the relative contents of 18:4, $18:3^{\omega 6}$, and $18:1^{\Delta 11}$ were twofold higher in the *pgd1* mutant than in the wild-type parental strain (Figure 5A). This was also seen in the total composition of all TAG acyl groups (Figure 4D). Interestingly, 18:4 and $18:3^{\omega 6}$ are mostly found in the extraplastidic lipids DGTS (see Supplemental Figure 2A online) and PtdEtn (see Supplemental Figure 2B online). Vaccenic acid ($18:1^{\Delta 11}$) is produced through elongation of $16:1^{\Delta 9}$, at least in plants (Nguyen et al., 2010), and is presumed to be extraplastidic. In view of an ~50% reduction of TAG in the *pgd1* mutant, the twofold relative increase in these three fatty acids suggests that the supply of TAG precursors from extraplastidic lipid turnover is not affected.

Precursor Fluxes from Plastid Lipids to TAG Are Reduced in *pgd1*

The analysis described above can only provide a static picture of lipid composition. However, the defect in a putative lipase-encoding gene in the *pgd1* mutant suggested that lipid remodeling or turnover might play a role in TAG accumulation in *C. reinhardtii* following N deprivation. To observe possible changes in the dynamics of lipid metabolism in the *pgd1* mutant, we employed pulse-chase labeling of membrane lipids using [^{14}C]-acetate, which can be converted easily to precursors of fatty acid biosynthesis in plastids. The labeling pulse was provided either before (150-min pulse duration; see Supplemental Figure 3 online) or during N deprivation (200-min pulse duration initiated 12 h after the start of N deprivation; Figure 6; see Supplemental Figure 4 online). Lipids were extracted as indicated and fractions of label incorporation into major lipids during the chase stage

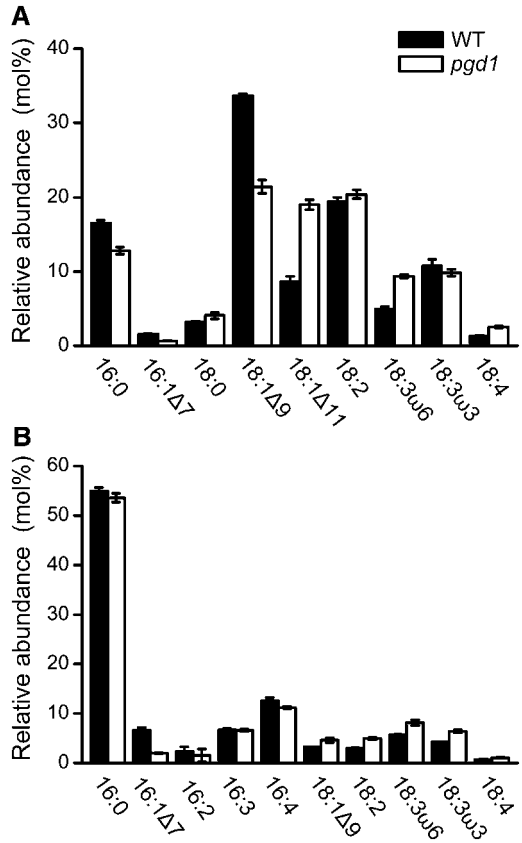

Figure 5. Positional Analysis of TAG Acyl Groups of the Wild-Type Parental Strain and *pgd1* Mutant 48 h after Transfer to N-Depleted Medium.

Purified TAG from *C. reinhardtii* cells was hydrolyzed by *R. arrhizus* lipase.

(A) Free fatty acids were presumed to be derived from *sn-1*/*sn-3* position of the glyceryl backbone of TAG. WT, the wild type.

(B) The residual monoacylglycerol contains the *sn-2* position acyl groups. The values represent the average of three replicates with error bars indicating SD.

were calculated. The difference in the incorporation of label into TAG between the wild-type parental strain and *pgd1* was more prominent when the labeling pulse was applied during N deprivation (Figure 6) compared with its application prior to N deprivation (see Supplemental Figure 3 online). This observation suggested that exchange of de novo–synthesized acyl groups through the membrane lipid pool into TAGs during N deprivation might involve PGD1, rather than the conversion of preexisting membrane lipids formed under N-replete conditions to TAGs. When the pulse was applied following N deprivation, plastid lipids, especially galactoglycerolipids, were rapidly labeled (Figure 6). Conditions were chosen such that the total label in the lipid extract during the chase phase remained approximately the same. In the wild-type parental strain, an increase of label in TAG was observed in parallel with a decrease of label in membrane lipids, suggesting the incorporation of acyl or diacylglyceryl groups derived from membrane lipids into TAGs. After 25 h of chase, the label remaining in membrane lipids was lower than that in TAGs. This situation was reversed in the *pgd1* mutant. In particular, the

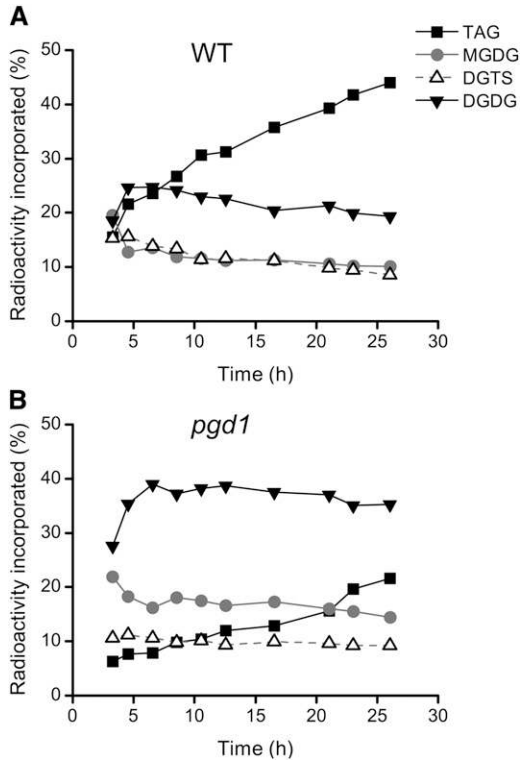

Figure 6. In Vivo Pulse-Chase Acetate Labeling of Lipids in the Wild-Type Parental Strain and the *pgd1* Mutant.

Labeled acetate was added 12 h following transfer of cells to TAP-N medium. The length of the [^{14}C]-acetate labeling pulse was 200 min, after which the cells were transferred to TAP-N medium lacking labeled acetate. Cells were collected at the times indicated, and lipid extracts were prepared and analyzed. The fraction of label in all analyzed lipids is given; lipids containing the bulk of the label and those most relevant for the discussion are shown in this figure. Fractions of label in other lipids are shown in Supplemental Figure 4 online. Lipid abbreviations are as defined for Figure 4. The data are from one representative experiment of a series of independent experiments. WT, the wild type.

fraction of label in the two galactoglycerolipids DGDG and MGDG remained much higher in *pgd1*. Because MGDG is its precursor, DGDG was labeled with some delay. In fact, it was the most highly labeled lipid in the *pgd1* mutant extracts, presumably because the transfer of labeled acyl or diacylglyceryl groups from MGDG into TAGs was disrupted in the mutant. When the pulse was applied prior to N deprivation (see Supplemental Figure 3 online), MGDG was the most highly labeled lipid, reflecting the fact that it is also the most abundant lipid under N-replete conditions, when TAG biosynthesis is repressed. Apparently, following N deprivation, de novo–synthesized acyl groups in the plastid are incorporated first into plastid membrane lipids, in particular MGDG, prior to becoming incorporated into TAGs, and the incorporation of acyl groups into TAG seems to require PGD1. Thus, MGDG serves as precursor for a fraction of acyl or diacylglycerol groups, those containing oleic acid (Figure 4), incorporated into TAGs following N deprivation. This process is disrupted in the mutant and more MGDG is converted to DGDG instead of TAG. PtdGro was rapidly turned over, but the rates of turnover remained approximately the same in the *pgd1* mutant and the wild type (see Supplemental Figure 4 online). Based on these data, we concluded that PGD1 might be a galactoglycerolipid lipase, prompting us to tentatively name the gene *PGD1*.

PGD1 Hydrolyzes Acyl Groups of MGDG with a Preference for the *sn-1* Position

To more directly determine the biochemical activity of PGD1, we produced the recombinant protein in *Escherichia coli*. The recombinant protein was affinity purified from denatured inclusion bodies (Figure 7A), renatured, and offered various substrate lipids in a lipase activity assay. To control for spontaneous lipid hydrolysis or lyso-lipid contamination, we assayed the protein refolding buffer without proteins. As a positive control, we assayed *R. arrhizus* lipase. We employed MGDGs of different molecular composition as substrates to determine the enzyme's preference. Mature MGDG was isolated from *C. reinhardtii* cells, which predominantly contains molecular species 18:3/16:4 (*sn-1*/*sn-2*). Using this substrate, the lyso-MGDG product that was generated was rather faint (Figure 7B). By analyzing the different fractions, we found that in the remaining MGDG after PGD1 hydrolysis, the 16:0 and 18:1$^{\Delta 9}$ acyl groups selectively disappeared, while the major acyl groups 16:4 and 18:3 remained (see Supplemental Figures 5A and 5B online). This suggested that PGD1 prefers to hydrolyze de novo–synthesized MGDG (18:1$^{\Delta 9}$/16:0), and the reaction stops when 18:1$^{\Delta 9}$/16:0 is depleted in the assay mixture. Hypothesizing that PGD1 only hydrolyzes de novo–formed MGDG to release 18:1$^{\Delta 9}$ for further TAG biosynthesis, reduction of 18:1$^{\Delta 9}$ in TAG of the *pgd1* mutant can be explained. The lyso-MGDG obtained using MGDG purified from *C. reinhardtii* exclusively contained 16:0 (see Supplemental Figure 5C online), suggesting that PGD1 prefers the *sn-1* position. However, the low amount of free fatty acids generated (see Supplemental Figure 5D online) made it difficult to draw a firm conclusion, considering that there may be lipids or fatty acids co-purified with the PGD1 protein.

To confirm that PGD1 prefers less desaturated molecular species, MGDG synthesized in *E. coli* by the activity of recombinant cucumber MGDG synthase (Shimojima et al., 1997) was used. In the buffer control lane, presumably no hydrolysis occurred as no generation of lyso-MGDG was seen (Figure 7B). This *E. coli*–derived MGDG band representing the substrate was isolated and shown to contain a combination of 18:1$^{\Delta 11}$, 16:0, or 16:1$^{\Delta 9}$ acyl groups (Figure 7D), which is similar to the newly assembled MGDG in *C. reinhardtii*. As indicated in Figure 7B by the intensity of the lyso-MGDG, PGD1 was more active on the MGDG species produced in *E. coli* using the cucumber (*Cucumis sativus*) MGDG synthase than the mature, mostly unsaturated MGDG from *C. reinhardtii*.

To obtain more information on the substrate preference of PGD1, we compared the acyl composition of the MGDG substrate, lyso-MGDG, and free fatty acid products that remained after incubation with the corresponding fractions obtained from *R. arrhizus* lipase hydrolysis. *R. arrhizus* lipase was inhibited by the buffer used for PGD1 refolding (Figure 7B). To generate lyso-lipid (including lyso-MGDG) standard, PBS instead of protein refolding buffer was used to dissolve *R. arrhizus* lipase for all the

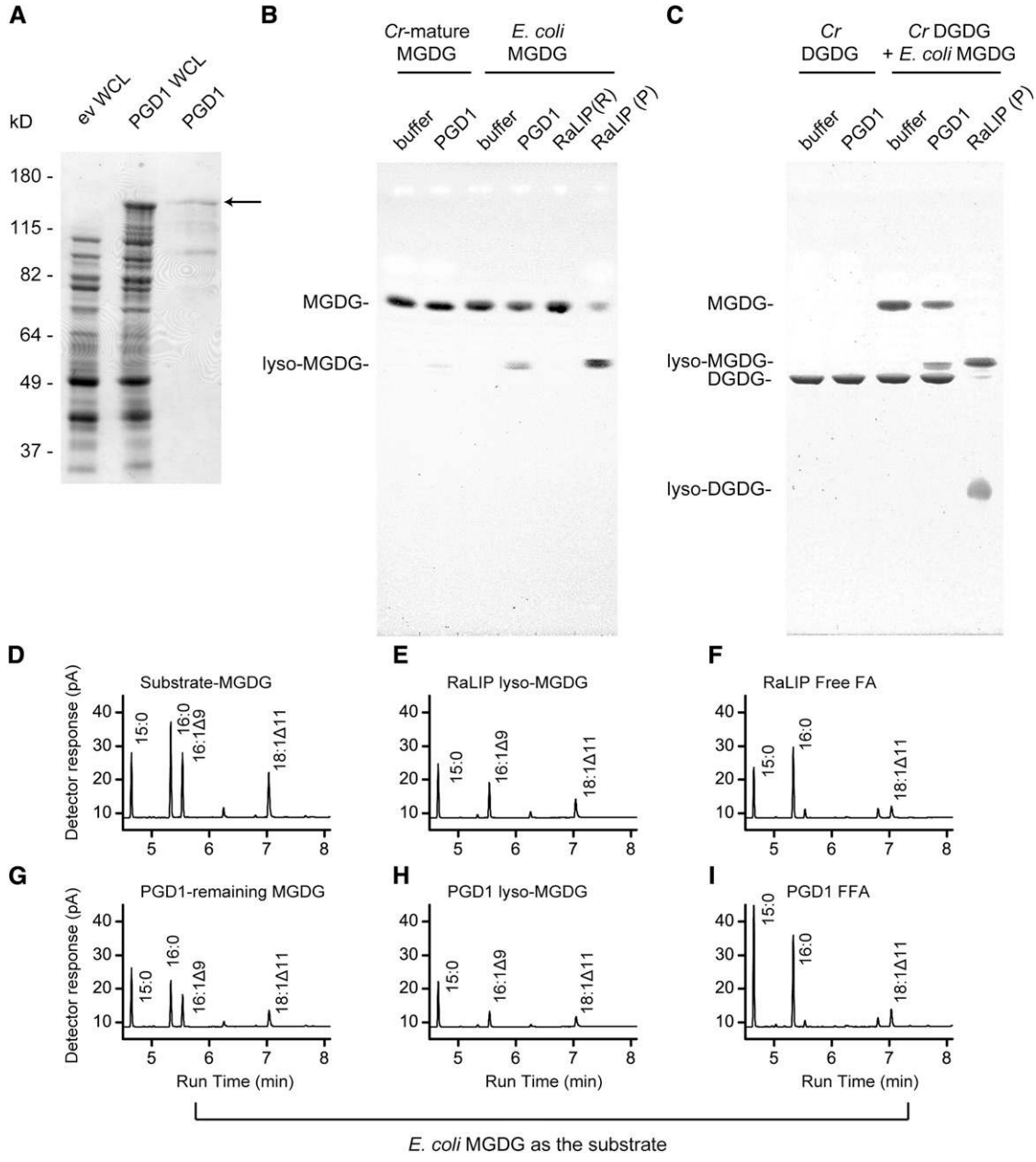

Figure 7. Activity of the Recombinant PGD1 Protein on MGDG and DGDG.

(A) SDS-PAGE of purified PGD1 protein and whole-cell lysates (WCL) from *E. coli* cells expressing the *PGD1* open reading frame and the empty vector control. Protein loading was 6 μg per lane for whole-cell lysates. Purified PGD1 protein loaded was 1 μg (quantified as in Methods; possibly biased by components in refolding buffer). Proteins were stained by Coomassie blue. The arrow indicates the PGD1 protein.

(B) A thin layer chromatogram of polar lipids from the lipase assay mixtures to which either mature MGDG extracted from *C. reinhardtii* (*Cr*) or MGDG extracted from the *E. coli* strain overexpressing cucumber MGDG synthase were added as substrates.

(C) A thin-layer chromatogram of polar lipids from the lipase assay mixtures to which either DGDG extracted from *C. reinhardtii* alone or mixed in with *E. coli*–derived MGDG at a 1:1 molar ratio were added as substrates. Glycolipids were visualized with α-naphtol reagent. Reaction products obtained with refolded PGD1 protein, blank refolding buffer, and *R. arrhizus* lipase dissolved in protein refolding buffer (RaLip-R) or PBS (RaLip-P) were analyzed.

(D) to **(I)** Gas–liquid chromatograms of methyl esters derived from a buffer control reaction containing *E. coli*–derived MGDG **(D)** or different fractions after lipase reaction with *E. coli*–derived MGDG as discussed in the text. As an internal standard, 15:0 was used. FA, fatty acid; FFA, free fatty acid.

reactions mentioned below. The *E. coli*–derived MGDG contains 16:0, 16:1$^{\Delta 9}$, and 18:1$^{\Delta 11}$ (Figure 7D, untreated sample) with 16:0 and 18:1$^{\Delta 11}$ present in the *sn-1* (Figure 7F) and 16:1$^{\Delta 9}$ and 18:1$^{\Delta 11}$ in the *sn-2* position (Figure 7E), as determined by *R. arrhizus* lipase digestion. After PGD1 hydrolysis, some of the substrate MGDG remained (Figure 7B). However, all the three major fatty acids were decreased to a similar extent (Figure 7G). Thus, the remaining MGDG was due to limited enzyme activity instead of the preference between different molecular species within *E. coli*–derived MGDG. Lyso-MGDG (Figure 7H) and free fatty acids (Figure 7I) generated by PGD1 resembled the corresponding fractions following *R. arrhizus* lipase digestion in fatty acid compositions, indicating that PGD1 prefers acyl groups at the *sn-1* position similar to *R. arrhizus* lipase.

We also explored the kinetics of PGD1-mediated hydrolysis of *E. coli*–derived MGDG. Lyso-MGDG was detectable in 30 min and continuously increased within 4.5 h of incubation (see Supplemental Figure 6A online). At 4.5 h, the bulk of MGDG substrate still remained, and we chose a 3-h incubation time to test the relationship between reaction velocity and substrate MGDG availability. It should be noted that MGDG is not soluble; therefore, classical enzyme kinetics is not directly applicable in this case. It should also be cautioned that the purified PGD1 enzyme went through a denaturation process, and the lipase activity may not be completely regained during refolding for all molecules present. Lyso-MGDG instead of free fatty acids was quantified because free fatty acids can be derived either from MGDG or lyso-MGDG. The hydrolysis of MGDG was linear in reaction velocity up to an apparent MGDG concentration of 300 μM (see Supplemental Figure 6B online).

PGD1 Does Not Act on DGDG

During the labeling experiment shown in Figure 6, labeling of DGDG increased to a greater extent in the *pdg1* mutant than did MGDG, suggesting that DGDG might be a possible substrate of PGD1. To test this possibility, DGDG extracted from *C. reinhardtii* was used as a substrate in the PGD1 assay. However, no formation of lyso-DGDG was detected by sugar-specific staining (Figure 7C). When *E. coli*–derived MGDG and *C. reinhardtii*–derived DGDG were offered in equal amounts, only lyso-MGDG was formed, showing that PGD1 used MGDG but not DGDG in this competition experiment, which might reflect the in vivo situation in which both lipids are present in the same membrane. While a single MGDG molecular species, 18:3/16:4, predominates in *C. reinhardtii* (see Supplemental Figure 2C online), DGDG is represented by a greater variety of molecular species with mostly 16:0 at the *sn-2* position and considerable amounts of 18:1$^{\Delta 9}$, 18:2, and 18:3 acyl groups present at the *sn-1* position of the glycerol moiety (Giroud et al., 1988) (see Supplemental Figure 2D online). Apparently, none of these DGDG molecular species is hydrolyzed by PGD1 under the conditions used. In addition, we tested PGD1 activity on other major membrane lipids prepared from *C. reinhardtii* extracts. PGD1-dependent generation of lyso-DGTS and lyso-PtdEtn was detectable by iodine staining, but at much lower levels than those generated by *R. arrhizus* lipase (see Supplemental Figures 7A and 7B online). Lyso-SQDG hydrolysis was not detectable by sugar-specific staining (see Supplemental Figure 7D online). Repeated trials of PtdGro hydrolysis by *R. arrhizus* lipase failed to yield an obvious lyso-PtdGro band (see Supplemental Figure 7C online), which is expected to run slower than PtdGro on TLC plates. This might be due to the fact that the *sn-2* position of PtdGro is composed of 16:0 and 16:1$^{\Delta 3}$ only (Giroud et al., 1988), while iodine stains lipids by binding to double bonds. Nevertheless, a major decrease in the lipid substrate after PGD1 hydrolysis was visible for *E. coli* MGDG (Figure 7B) but not PtdGro nor DGTS, PtdEtn, and SQDG. At this time, synthetic molecular species are not available for lipids such as MGDG and DGTS. Thus, we were unable to compare lipids with exactly the same acyl compositions but different head groups.

The *pgd1* Mutant Loses Viability Following N Deprivation

In contrast with the wild-type parental strain, *pgd1* mutant liquid cultures and colonies on agar-solidified medium became chlorotic 5 to 9 d following N deprivation (Figures 1C and 8A). We took advantage of this observation during the complementation analysis described above. The increasing chlorosis correlated well with the decrease in the chlorophyll content (Figure 8B) as well as the decline in the viability of *pgd1* following N deprivation (Figure 8C). Following N deprivation *C. reinhardtii* typically ceases cell growth after approximately one cell cycle (Work et al., 2010; James et al., 2011). However, these cells continue to capture light with their photosynthetic light-harvesting complexes. If electron acceptors become limiting due to the cessation of growth under these conditions, photosynthetic electron transport chain components may become overreduced. Indeed, it has been hypothesized that enhanced fatty acid synthesis and sequestration of acyl groups in TAG provide an electron sink because acyl groups are among the most reduced carbon compounds that algae can produce (Hu et al., 2008). A potential consequence of TAG deficiency is the increase in the NADPH/NADP$^+$ ratio. This is because NADPH is a major reductant in fatty acid synthesis. With decreasing availability of NADP$^+$, molecular oxygen may become an alternative electron acceptor for photosystem I. Thus, when photosynthetic electron transport exceeds the capacity of the NADP$^+$ pool to accept electrons in *pgd1* due to decreased TAG synthesis, a superoxide may be generated and further converted to H_2O_2 and hydroxyl radicals (Mehler, 1951). Overproduction of these highly cytotoxic reactive oxygen species (ROS) may lead to cell death. To begin to test this hypothesis, we took advantage of the herbicide 3-(3,4-dichlorophenyl)-1,1-dimethylurea (DCMU), which specifically inhibits photosynthetic electron transfer at the acceptor side of photosystem II (Draber et al., 1970). DCMU treatment is well known to decrease the generation of superoxide and other ROS from photosystem I (Davies et al., 1996; Wen et al., 2008; Robert et al., 2009). When DCMU was added to N-deprived cultures, chlorosis and viability loss were suppressed (Figures 8A to 9C). To further verify this hypothesis, we analyzed thiobarbituric acid reactive substances (TBARS), a product of ROS (Baroli et al., 2003), and observed a burst of TBARS in the *pgd1* mutant, which was also reverted by DCMU (Figure 8D). As expected, DCMU did not rescue the *pgd1* TAG phenotype but did decrease TAG levels of the wild-type parental strain (Figure 8E) because of the decrease in electrons provided for NADPH generation.

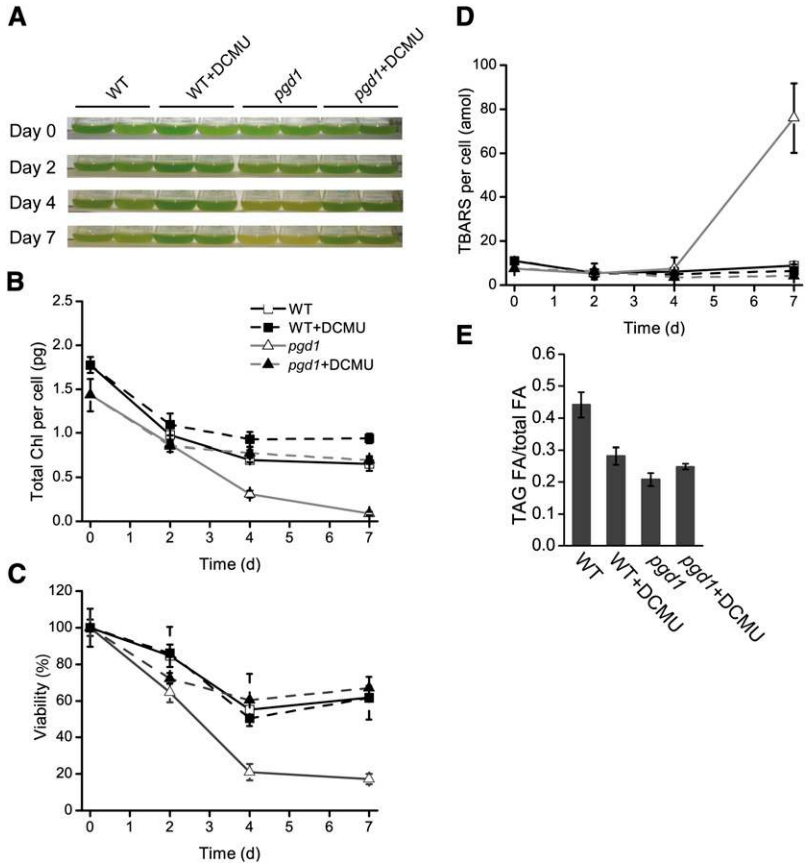

Figure 8. Biochemical and Physiological Characterization of Wild-Type Parental Strain and the *pgd1* Mutant Following N Deprivation.

(A) Appearance of cultures grown in TAP-N for the number of days indicated. The electron transport chain inhibitor DCMU dissolved in DMSO was present at a final concentration of 2 μM as indicated. Two representative cultures per line are shown. WT, the wild type.

(B) Time course of total cellular chlorophyll (Chl) content.

(C) Time course of cell viability relative to day 0, the start of N deprivation following transfer to TAP-N medium.

(D) Time course of cellular TBARS content.

(E) TAG accumulation presented as ratio of fatty acids (FA) in TAGs over total fatty acids in the lipid extracts after 2 d of N deprivation. For all quantitative data, three replicates were averaged, with SD indicated by the error bars.

DISCUSSION

The primary phenotype through which the *pgd1* mutant was identified is a reduction in the accumulation of TAGs following N deprivation (Figure 1). Because the affected gene, *PGD1*, encodes a galactoglycerolipid lipase with preference for the *sn-1* position of the respective glyceryl backbone (Figure 7), we had to reconsider how TAGs are synthesized in *C. reinhardtii*. A mechanistic model that accommodates our current findings on the *pgd1* mutant and the PGD1 protein and that places PGD1 into the context of overall cellular lipid metabolism is shown in Figure 9. Because the *pgd1* mutant still accumulates considerable amounts of TAGs, additional pathways not involving PGD1 are contributing to TAG accumulation in N-deprived cells. For the purpose of simplification, Figure 9 shows a single lipid droplet receiving TAG assembled at the ER or the plastid envelopes. The process can be divided into two conceptual phases that will be discussed separately: First, the photosynthetic generation of reductant for fatty acid biosynthesis; and second, the incorporation of acyl groups into TAGs, which we will discuss first.

An MGDG Deacylation/Acylation Cycle Involved in TAG Biosynthesis of *C. reinhardtii*

Figure 9 summarizes our current working hypothesis of PGD1 function in TAG metabolism. We placed the galactoglycerolipids, in particular MGDG, at the center of the plastid envelope pathway as our pulse-chase experiment (Figure 6) suggested that acyl groups or entire DAG moieties move through the membrane lipid fraction of the chloroplast prior to incorporation into TAGs. In the *pgd1* mutant, the labeling of galactoglycerolipids was increased, but the relative amounts of the membrane lipid classes did not change. Apparently, the pool size of MGDG and other membrane lipids is strictly controlled to maintain functional photosynthetic membranes.

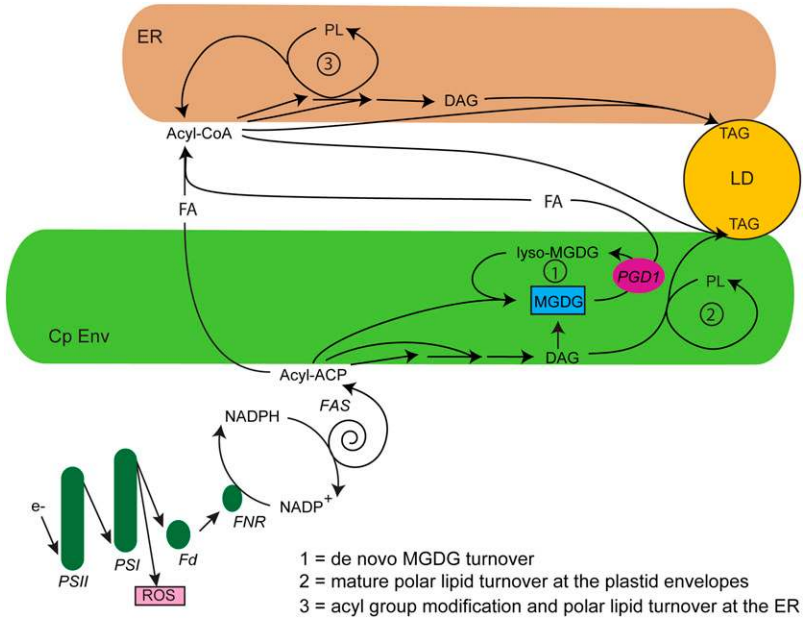

Figure 9. Hypothesis Placing PGD1 into the Context of Overall Cellular Lipid Metabolism Explaining Its Role in TAG Biosynthesis.

For simplicity, a single lipid droplet (LD) is shown forming at the ER or the chloroplast envelope (Cp Env). Thylakoid membranes harboring the two photosystems have been omitted. Three lipid turnover processes discussed in the text are indicated by numbers: 1, turnover of newly synthesized MGDG; 2, turnover of mature MGDG and other thylakoid lipids at the plastid envelopes; 3, acyl group modification and lipid turnover at the ER. Enzymes, protein complexes, and processes are italicized: FAS, fatty acid synthase complex; Fd, ferredoxin; FNR, ferredoxin:NADP$^+$ reductase; PSI and II, photosystems I and II. Substrates and products are as follows: DAG, diacylglycerol; e-, electron; FA, fatty acid; PL, polar lipids. Not all intermediates or reactions involved are shown.
[See online article for color version of this figure.]

The importance of galactoglycerolipids in TAG metabolism in *C. reinhardtii* may arise from the fact that this alga lacks PtdCho (Giroud et al., 1988). PtdCho is one of the most rapidly labeled and metabolized membrane lipids in seed plants, and acyl exchange involving PtdCho has been suggested to play a role in the export of fatty acids relevant for extraplastidic membrane lipid biosynthesis, including that of TAGs (Bates et al., 2007, 2009). *C. reinhardtii* membranes contain the betaine lipid DGTS, which has been widely assumed to play at least some of the roles of PtdCho in *C. reinhardtii* due to similarities in structure and biophysical properties of the two lipids (Sato and Murata, 1991). However, our labeling and lipid analysis data showed no differences for DGTS between the parental strain and the *pgd1* mutant and suggested it is not involved, at least in the aspect of TAG biosynthesis that is affected in the *pgd1* mutant. Although DGTS and PtdEtn molecular species isolated from *C. reinhardtii* were hydrolyzed by recombinant PGD1 to a limited extent (see Supplemental Figures 7A and 7B online), DGTS and PtdEtn showed the same change in molecular species composition in the mutant (i.e., the reduction of oleic acid containing species) (Figure 4; see Supplemental Figure 2 online), as was seen also for TAGs. It should be noted that DGTS and PtdEtn are extraplastidic membrane lipids. Oleate (18:1$^{\Delta 9}$) and palmitate (16:0) typically are the de novo–synthesized acyl groups incorporated into the glyceryl backbone. Thus, the reduction of oleate in TAG in *pgd1* suggests that the TAG affected in this mutant is derived from glyceryl moieties containing these de novo–synthesized acyl groups. Pulse-chase labeling data obtained when labeled acetate was added prior to N deprivation showed few differences between the mutant and the parental strain (see Supplemental Figure 3 online). However, stark differences were observed when the pulse was given following N deprivation (Figure 6), suggesting that the fraction of TAG requiring PGD1 activity indeed involves de novo fatty acid biosynthesis.

As DGTS and PtdEtn in the *pgd1* mutant are likely downstream products of PGD1 activity, just like TAG as discussed above, it seems probable that a plastid lipid serves as the true substrate for PGD1 and that PGD1 may be involved in cycling newly synthesized fatty acids through the plastid polar lipid pool. DGDG is not likely a major substrate for PGD1 in cells as it is also not a substrate for PGD1 in vitro, even though it is highly labeled during pulse-chase experiments in the *pgd1* mutant (Figure 6). The delay in labeling of DGDG compared with MGDG is consistent with biosynthesis of DGDG by galactosylation of MGDG. Thus, if cycling of acyl groups into TAG through the MGDG pool is reduced in *pgd1*, the reduced flux from MGDG to TAG allows for greater availability of MGDG for DGDG biosynthesis, explaining increased labeling of this lipid in the mutant.

In vitro lipase assays suggested that PGD1 prefers MGDG over DGDG, with a preference for MGDG molecular species with fewer double bonds over 18:3/16:4 species, and a preference for acyl groups at the *sn-1* position over *sn-2*. To explain these observations, we propose an acyl-editing cycle (Figure 9, process 1) involving MGDG assembled from de novo–synthesized

fatty acids (18:1$^{\Delta 9}$/16:0). One function of such a cycle involving a transient MGDG pool might be the transfer of fatty acids synthesized in the plastid through the plastid envelope membranes effectively accomplishing a net export of 18:1$^{\Delta 9}$ acyl groups. As 18:1$^{\Delta 9}$ is a major fatty acid in TAG (Figure 4D), but not in DGTS or PtdEtn (see Supplemental Figures 2A and 2B online), TAG is most affected of the extraplastidic lipids in the *pgd1* mutant. Interestingly, in the *pgd1* mutant MGDG did not accumulate 18:1$^{\Delta 9}$ (see Supplemental Figure 2C online) but apparently continued to become desaturated to its mature 18:3/16:4 molecular species. Alternatively, it seems likely that MGDG assembly from newly synthesized acyl groups is feedback inhibited, adjusting the flow through the pathway to the demands of the cell. Thus, the total amount of fatty acids in the *pgd1* mutant is lower than in the wild-type parental strain (Figure 4C), and the relative amount of 18:1$^{\Delta 9}$ in the total lipid extracts is reduced (Figure 4D).

Mature MGDG found in thylakoid membranes is predominantly composed of the 18:3/16:4 species (see Supplemental Figure 2C online). Perhaps the presence of the unusual 16:4 acyl group, or other highly unsaturated acyl groups, protects MGDG from degradation by PGD1 because it is a necessary building block of the photosynthetic membrane, while allowing cycling of de novo–synthesized acyl groups through the MGDG pool. This process is not perfect as 18:3 and 16:4 acyl groups were present in TAGs of the wild-type parental strain or the *pgd1* mutant, indicating some turnover of mature MGDG (Figure 9, process 2). It is likely that following severe N deprivation, photosynthetic membranes containing mature MGDG species are degraded to some extent, perhaps involving lipases different from PGD1, and that these acyl or diacylglycerol moieties find their way into the TAG fraction. But the bulk of the membrane has to be maintained for a rapid recovery when nitrogen is resupplied. Thus, the resistance of mature *C. reinhardtii* MGDG to PGD1-catalyzed hydrolysis supports the hypothesis of de novo–synthesized acyl group cycling through a specific MGDG subpool. For this hypothesis to be valid, an acyl-ACP:lyso-MGDG acyltransferase activity is required for acylation of lyso-MGDG. Such an enzyme activity with a preference for the *sn-1* position has been described for a cyanobacterium (Chen et al., 1988). We assume that *C. reinhardtii* has an ortholog, although the identity of the gene is not yet known.

One possible shortcoming of the proposed hypothesis is that no chloroplast transit peptide was predicted for PGD1, suggesting it to be extraplastidic. However, a cytosolic location would give PGD1 access to MGDG in the outer leaflet of the outer membrane, where this lipid has been shown to be present (Joyard et al., 1991). Analogously, the outer envelope protein, SFR2, of *Arabidopsis* (Moellering et al., 2010) acts on MGDG, suggesting that PGD1 has access to MGDG molecules in the outer envelope, even if it is not inside the plastid. We attempted to resolve this issue, but subcellular localization of PGD1 using green fluorescent protein fusion constructs was unsuccessful. Alternative localization approaches, such as immunolocalization of PGD1, will have to await the availability of antibodies.

How Does Oleate Availability Affect TAG Biosynthesis?

The fatty acid composition of TAG of the *pgd1* mutant (Figures 4D and 5) lacks18:1$^{\Delta 9}$ and has a higher relative abundance of 18:1$^{\Delta 11}$, 18:3$^{\omega 6}$, and 18:4 acyl groups. To explain these observations, we considered the different sources for acyl groups that might be present in TAGs: (1) de novo synthesis (Figure 9, process1), for which 18:1$^{\Delta 9}$ is the diagnostic fatty acid most increased following N deprivation (Figure 4D); (2) plastid membrane lipid degradation (Figure 9, process 2) indicated by the presence of 16:4 and 18:3$^{\omega 3}$ in TAGs derived from mature MGDG; and (3) extraplastidic membrane lipid modification and turnover (Figure 9, process 3) characterized by the presence of 18:1$^{\Delta 11}$, 18:3$^{\omega 6}$, and 18:4 acyl groups in TAG. Fatty acids such as 16:0 can be derived from multiple processes and therefore are not diagnostic. The DAG backbone for most TAG species originates from the chloroplast pathway since the *sn-2* position of TAGs of *C. reinhardtii* contains up to 80% 16-carbon fatty acids (Figure 5) (Fan et al., 2011). We suggest that the plastid DAG pool primarily contributes to TAG biosynthesis. Plastid DAG can derive from both de novo assembly and plastid membrane lipid degradation (Figure 9, process 2). Turnover of de novo–synthesized MGDG (Figure 9, process 1) will contribute to the cytosolic acyl-CoA pool, which provides acyl groups for the *sn-3* position in TAGs. Similarly, lipid modification and turnover at the ER (Figure 9, process 3) likely provide acyl-CoA substrate for the diacylglycerol acyltransferase. The absence of PGD1 impairs the export of 18:1$^{\Delta 9}$ with two consequences: decrease of 18:1$^{\Delta 9}$-CoA as substrate for TAG biosynthesis (Figure 4D) and decrease of 18:1$^{\Delta 9}$ in the DAG backbones of DGTS and PtdEtn (see Supplemental Figures 2A and 2B online).

Among the fatty acids bound in TAG, the relative amounts of those from extraplastidic membrane lipid turnover (18:1$^{\Delta 11}$, 18:3$^{\omega 6}$, and 18:4) were doubled in the *pgd1* mutant (Figures 4D and 5). Considering the approximately twofold decrease in TAG content in the *pgd1* mutant, this can be explained by the fact that extraplastidic membrane lipid turnover (Figure 9, process 3) was not affected by the *pgd1* mutation, while the total TAG amount was decreased twofold.

By contrast, the relative amounts of fatty acids provided by mature plastid membrane lipid turnover (16:4 and 18:3$^{\omega 3}$) remained the same or only slightly increased (Figures 4D and 5). Therefore, the absolute amounts of these two fatty acids in TAGs were decreased.

TAG Accumulation Protects Cells from Oxidative Damage

The accumulation of TAG by microalgae following nutrient deprivation has been repeatedly documented over many years, but experimental exploration of the physiological role of this process has been scarce. The availability of the *pgd1* mutant with reduced oil content now provides an excellent opportunity to explore the function of TAG accumulation in microalgae. One can postulate that TAG is synthesized following N deprivation to store excess carbon when amino acid synthesis becomes impaired, an important but possibly not essential role for TAG accumulation, because photosynthate could presumably also be partitioned into increasing amounts of carbohydrates. However, the major loss in viability of *pgd1* (Figure 8C) suggests that TAG accumulation is essential for cells to survive following N deprivation. This observation provides direct experimental verification for recent suggestions that TAG might serve as an outlet to sequester excess electrons

moving through the photosynthetic electron transport chain (Hu et al., 2008), thereby preventing the reduction of molecular oxygen and generation of ROS, which are cytotoxic. The connection between photosynthetic electron transport and TAG metabolism is shown in Figure 9. In the wild-type parental strain, photosynthetic electron flow supplies the reducing equivalents in the form of NADPH for fatty acid synthesis. If electron transport is blocked with DCMU, the reduced electron flow into the NADPH pool would limit TAG biosynthesis resulting in lower levels of TAG (Figure 8E) as was recently also observed by others (Fan et al., 2012). However, if TAG biosynthesis is compromised as in *pgd1*, molecular oxygen probably serves as an alternative electron acceptor leading to the formation of excess ROS and ultimately cell death. DCMU treatment of *pgd1* relieves the production of ROS by decreasing the electron flow to molecular oxygen.

The assay employed to detect TBARS is commonly used to measure the consequences of oxidative stress in *C. reinhardtii* (Baroli et al., 2003; Fischer et al., 2007). As products of lipid peroxidation, TBARS are easier to detect than ROS themselves, which are short-lived (Shulaev and Oliver, 2006). We observed a strong accumulation of TBARS in the *pgd1* mutant on day 7 of N deprivation (Figure 8D). However, this effect was preceded by the loss of ability to form colonies indicating a loss in cell viability (Figure 8C). Similarly, Baroli et al. (2004) tested the ability to form colonies and TBARS accumulation in a *C. reinhardtii* mutant sensitive to high light and observed a similar lag in TBARS formation. It is likely that lower amounts of ROS can cause loss of colony forming ability, while the formation and accumulation of detectable levels of TBARS requires more time. However, we cannot exclude the alternate explanation that cell death itself is the cause of TBARS accumulation in the *pgd1* mutant.

If the proposed hypothesis that TAG biosynthesis mitigates ROS formation at photosystem I following N deprivation is correct, we expect to identify more mutants deficient in TAG accumulation that lose viability following N deprivation. In fact, the essentiality of TAG accumulation opens new opportunities for additional forward genetic screens of mutants compromised in genes required for TAG biosynthesis and its regulation or even photosynthetic electron transport.

Conclusions

The isolation of the *pgd1* mutant led to the discovery of a galactolipid lipase that plays a role in TAG accumulation following N deprivation in *C. reinhardtii*. This finding was not predicted based on our current knowledge of lipid metabolism in seed plants. However, *C. reinhardtii* lacks PtdCho, which is the polar lipid in plants on which the modification of acyl groups followed by acyl exchange happens. Thus, one might wonder whether the TAG assembly pathway presented here is specific to *C. reinhardtii*. A cursory check suggests that there are possible orthologs of PGD1 in plants and other algae and that the hypothesis outlined in Figure 9 may therefore also have some relevance to TAG biosynthesis in plants and other algae, at least under certain growth conditions and perhaps with modifications.

The *pgd1* mutant also provides the means to experimentally demonstrate a long postulated role of TAG accumulation following nutrient deprivation in microalgae. Apparently, TAG accumulation relieves the reducing pressure on the electron transport chain under nutrient stress conditions when cells stop growing but still photosynthesize and possibly alleviates the production of harmful ROS, which can result in cell damage. Ultimately, a better understanding of the assembly pathways for TAG and the physiological consequences of TAG accumulation will help shape our thinking of how to engineer improved algal feedstock for fuel, feed, and industrial chemicals.

METHODS

Strains and Growth Conditions

The cell wall–less dw15-1 (cw15, nit1, mt^+) strain of *Chlamydomonas reinhardtii* was obtained from A. Grossman and is referred to as the wild type (with regard to *PGD1*) parental strain throughout. This strain was crossed to CC-198 (er-u-37, str-u-2-60, mt^-; Chlamydomonas Resource Center, http://www.chlamycollection.org) for genetic analysis. Cells were grown in Tris-acetate-phosphate (TAP) medium (20 mM Tris, 0.1 g/L $MgSO_4$ $7H_2O$ [0.4 mM], 0.05 g/L $CaCl_2$ $2H_2O$ [0.34 mM], 10 mL/L glacial acetic acid, 10 mM NH_4Cl, 1 mM phosphate, and trace elements [Harris, 1989]) under continuous light (70 to 80 μmol m^{-2} s^{-1}) at 22°C or ambient room temperature (~22°C) for solid media, which contained 1.5% agar. Ammonium chloride was omitted from N-depleted (TAP-N) medium. To induce TAG biosynthesis, cells were collected by centrifugation (3000*g*, 4°C, 3 min), washed twice with TAP-N, and finally resuspended in TAP-N of the same volume. For spotting on TAP-N agar, ~10^6 cells from a log-phase culture were concentrated in 5 μL.

Primary Mutant Screen

Plasmid disruption was used to generate mutants of the wild-type parental strain dw15-1. Transformation using glass beads was performed as previously described (Kindle, 1990) using the pHyg3 plasmid conferring resistance to hygromycin B (Berthold et al., 2002). The plasmid was linearized with *Nde*I (all the restriction endonucleases were purchased from New England Biolabs). After 8 h of recovery, cells were spread onto agar-solidified TAP medium containing 10 μg/mL hygromycin B. Colonies were picked into 96-well plates with 1.1 mL of TAP medium and grown for 3 d. For N deprivation and induction of TAG biosynthesis, small culture droplets (~3 μL) were transferred with a 48-pin replicator to inoculate a new 96-well plate containing TAP medium containing 0.5 mM ammonium chloride and grown for 6 to 7 d under continuous light (70 to 80 μmol m^{-2} s^{-1}) at ambient room temperature (~22°C). For normalization within a 96-well plate, chlorophyll fluorescence was used. For this purpose, 100 μL of N-deprived cells was transferred to a black 96-well plate (Black Flat Bottom Polystyrene NBS Microplate 3991; Corning) and read at 455-nm excitation with an emission filter cutoff >685 nm using a FLUOstar Optima 96-well plate reader (BMG Labtech). In the same plate to visualize neutral lipids, 100 μL Nile Red stock solution (Sigma-Aldrich) (5 μg/mL in 10% methanol containing 0.04% Triton X-100) was added. The wavelength settings for Nile Red fluorescence were 455 nm for excitation and 550 to 560 nm for emission. A background reading for this filter set was obtained prior to the addition of Nile Red (cells only) and subtracted. The neutral lipid-specific signal was calculated as [(Nile Red fluorescence – background fluorescence)/chlorophyll fluorescence]. To identify outliers in individual 96 plate sets, the median absolute deviation (MAD) was determined as [1.482 × median × |individual value-median|] according to Rousseeuw and Croux (1993), and the z-score was calculated as [(individual value-median)/MAD] as previously described for another mutant screen (Lu et al., 2008). The threshold for the z-score was set at ± 3.

Genetic Analysis

In preparation for crossing, the *pgd1* mutant in the dw15-1 background and CC-198 were separately grown for 5 d on TAP with 4 g/L yeast extract, transferred with a sterile loop to TAP agar with 10% the normal concentration of N for 2 d, and then suspended at high density in test tubes with sterile water and placed on a shaker overnight. On the following day, the two cell types were combined using 0.5-mL aliquots, removed after 2 to 3 h of mating, and plated onto TAP medium completely lacking N and solidified with 4% agar. After 1 d in the light, the zygote plates were moved to the dark. Five days after mating, zygospores were sampled as described by Harris (1989). On the day following transfer of the zygospores to normal TAP solidified with 2% agar, meiotic progeny were identified under a dissecting microscope and separated with a glass needle. After 7 d, the colonies were sufficiently large to transfer to nonselective media for subsequent replica plating.

DNA and RNA Techniques

Genomic DNA of *C. reinhardtii* was prepared according to Newman et al. (1990). For DNA gel blotting, genomic DNA was digested with *Bam*HI and resolved by agarose gel electrophoresis (10 μg DNA per lane). DNA was transferred to a nylon membrane (Amersham Hybond N^+; GE Healthcare) and fixed under UV light. Digoxigenin labeling of the probe, DNA transfer, and signal detection were performed using a kit from Roche following the manufacturer's instructions. The probe was generated through PCR amplification of a 234-bp region within the hygromycin B resistance cassette with primers SF and SR (all primer sequences can be found in Supplemental Table 1 online).

For genotyping and SiteFinding PCR (Tan et al., 2005), Taq polymerase (Invitrogen) was used. For genotyping, the PCR conditions were according to the protocol provided by Invitrogen with primers F1, S2-1, and R. SiteFinding PCR was conducted according to (Tan et al., 2005) with minor modifications and with primers optimized for the pHyg3 plasmid. The primers used for finding the insertion in *PGD1* were SiteFinder6 in combination with S1-1 and S1-2 and SiteFinder8 in combination with S2-1 and S2-2. In addition, nested primers SFP1 and SFP2 were used for both combinations.

RNA was isolated using the RNeasy plant mini kit (Qiagen) according to the manufacturer's instructions. To obtain cDNA as the template for RT-PCR, RNA was subjected to reverse transcription with Superscript II reverse transcriptase (Invitrogen). For real-time PCR, the commonly used reference gene *RACK1* was employed for normalization using previously reported primers (Chang et al., 2005). Primers used for *PGD1* were qF and qR. Data were analyzed with the $2(-\Delta\Delta C(T))$ method (Livak and Schmittgen, 2001).

For expression of *PGD1* in *Escherichia coli*, cDNA was originally amplified with primers CF1 and CR1 using the Failsafe PCR kit from Epicentre. The PCR product was then integrated into the *Not*I-linearized yeast vector pMK595 (Luo et al., 2010) by homologous recombination in *Saccharomyces cerevisiae* (Ma et al., 1987). The fusion plasmid was recovered by transforming *E. coli* with yeast DNA extract and designated pXL1238. This plasmid was then used as a template for PCR using primers CF2 and CR2 and Phusion polymerase (New England Biolabs) to generate a fragment with *Bam*HI and *Sal*I sites. The PCR product was ligated into pCR-Blunt (Invitrogen) and cut out with *Bam*HI and *Sal*I. This fragment was ligated into pLW01-DsRed (Lu and Benning, 2009) to generate plasmid pXL1256. pXL1256 was sequenced and mutations were found. The mutated region was removed by restriction digestion, and the remaining backbone was ligated with digested RT-PCR product of that region to obtain plasmid pXL1262. Another PCR was performed to amplify PGD1 cDNA from pXL1262 using primers CF3 and CR3. PCR product and an expression vector pMK1006 (provided by M.-H. Kuo) were combined using a ligation-independent cloning procedure (Aslanidis and de Jong, 1990) and sequenced for confirmation. In this plasmid, *PGD1* expression was under the control of a T7 promoter and the resulting fusion protein was N-terminally tagged with poly-His.

Mutant Complementation

A cotransformation protocol was used to introduce wild-type sequences into the *pgd1* mutant in the dw15-1 (nit-) background. Plasmid pMN24 (Fernández et al., 1989) containing the *C. reinhardtii* nitrate reductase gene *NIT1* as selection marker was digested with *Bam*HI and used for glass bead transformation of the *pgd1* mutant. A BAC 5E6 containing wild-type genomic DNA was obtained from the Clemson University Genomics Institute and was digested with *Kpn*I and *Ase*I to excise a 9.5-kb fragment containing the *PGD1* genomic DNA. In each transformation, 0.25 μg linearized pMN24 and 0.3 μg gel-purified BAC fragment were used. TAP plates containing 0.5 mM nitrate instead of 10 mM ammonium were used for selection. The nitrate served initially as the nitrogen source, and the low concentration led eventually to conditions of N deprivation and chlorosis of the *pgd1* mutant but not complemented lines or the wild-type parental control. After transformation of *pgd1* with pMN24, colonies from noncomplemented lines formed and bleached within ~3 weeks when grown under continuous light (70 to 80 $\mu mol\ m^{-2}\ s^{-1}$) at ambient room temperature (~22°C). Complemented lines forming green colonies were restreaked and maintained on agar-solidified TAP medium with 10 mM nitrate as the sole N source to avoid growth of potentially contaminating nontransformed cells.

Lipid Analysis and Pulse-Chase Labeling

Lipid extraction, TLC of neutral lipids, transesterification, and gas–liquid chromatography were done according to Moellering and Benning (2010). Briefly, lipids were extracted from cell pellets with methanol, chloroform, and 88% formic acid (2:1:0.1 by volume). To the extract, 0.5 volume of 1 M KCl and 0.2 M H_3PO_4 was added and mixed, and phases were separated by low-speed centrifugation. For TAG quantification, lipids were resolved by TLC on Silica G60 plates (EMD Chemicals) developed in petroleum ether-diethyl ether-acetic acid (80:20:1 by volume). Polar lipids were separated on the same plate using chloroform-methanol-acetic acid-water (75:13:9:3 by volume) as solvent. To analyze lyso-glycolipids for the PGD1 assay, acetone-toluene-water (91:30:7.5 by volume) was used instead. Brief exposure to iodine vapor was employed for visualization of lipids. Transesterification of each lipid and separation of fatty acid methyl esters by gas–liquid chromatography were as previously described (Rossak et al., 1997). Transesterification was conducted on pellets with a known number of cells to determine the cellular total fatty acid content. Staining with α-naphtol (Benning et al., 1995) was used for the PGD1 assay to detect galactoglycerolipids.

For pulse-chase labeling experiments, cells were grown to log phase in TAP medium and either used directly (see Supplemental Figure 3 online) or transferred to TAP-N medium and grown for 12 h to induce N deprivation. Cells were harvested and resuspended at a concentration of 3 to 8×10^8 per mL either in modified TAP (see Supplemental Figure 3 online) or TAP-N medium (Figure 6; see Supplemental Figure 4 online) containing 6 mM acetate (normal TAP contains 17.5 mM). To these cultures [^{14}C-U]-acetate (specific activity 45-60 mCi/mmol; Perkin Elmer) was added to provide 1 μCi/mL. In a typical experiment after 1 to 4 h of incubation in the light, 20 to 40% of the labeled acetate was incorporated as determined by liquid scintillation counting. At the end of the pulse labeling phase, cells were centrifuged and washed to remove the labeled acetate, and cells were resuspended in TAP-N containing the normal amount of acetate to initiate the chase phase. Lipid extracts were prepared as described above, split in half, and analyzed for polar lipids DGTS, PtdEtn, MGDG, DGDG, PtdGro, and a mixture of SQDG and phosphatidylinositol, which could not be individually analyzed due to their low total amount in this

experiment. Material at the origin of the TLC was also analyzed and included. The other half of the sample was analyzed for nonpolar lipids DAG and TAG. Lipids were isolated from the TLC plates, and incorporation of label into each lipid was quantified by scintillation counting. These lipid fractions were summed up, and percentages for each lipid fraction were calculated.

Recombinant Protein Production and PGD1 Assay

BL21 (codon+) *E. coli* strains harboring the empty pMK1006 vector or the pMK1006-*PGD1* construct were grown to log phase at 37°C. Isopropyl-β-D-thiogalactopyranoside was added to the final concentration of 0.5 mM to induce protein production. Cells were harvested after 3 h of induction. To extract proteins, cells were resuspended in lysis buffer (20 mM Tris-HCl, pH 7.9, 10% glycerol, 150 mM NaCl, and 1 mM DTT). The mixture was then frozen in liquid nitrogen and thawed at room temperature for three cycles and sonicated to lyse cells. Lysates were centrifuged at 21,000*g* for 15 min to obtain inclusion bodies. Inclusion bodies were washed with 5 mL/g wash buffer (4 M urea, 0.5 M NaCl, 1 mM EDTA, 1 mg/mL sodium deoxycholate, and 50 mM Tris-Cl, pH 8.0) twice and denatured with solubilization buffer (8 M urea, 50 mM Tris-Cl, pH 8.0, and 10 mM DTT) by incubation at 50°C for 20 min. Supernatant was collected after centrifugation at 21, 000*g* for 30 min and subjected to nickel-nitrilotriacetic acid affinity purification as described before (Lu and Benning, 2009). His-tagged PGD1 protein was eluted with solubilization buffer containing 200 mM imidazole. Aliquots of purified proteins were diluted in 15 different buffers of the QuickFold Kit (AthenaES), assayed for lipase activity, and 40× dilution into protein refolding buffer (50 mM Tris-Cl, pH 8.5, 9.6 mM NaCl, 0.4 mM KCl, 1 mM EDTA, 0.5 M Arg, 0.75 M guanidine-HCl, 0.05% polyethylene glycol 3350, and 1 mM DTT) was found to be optimal for PGD1. After 1 h incubation at 4°C, proteins were aliquoted and kept frozen at −80°C. Protein concentration was determined with Bio-Rad protein assay dye reagent concentrate according to the manufacturer's instructions.

To prepare lipid substrates from *C. reinhardtii* or *E. coli* cells, lipids were extracted from 48 h N-deprived *C. reinhardtii* cells or isopropyl-β-D-1-thiogalactopyranoside-induced *E. coli* cells expressing cucumber (*Cucumis sativus*) MGDG synthase (Shimojima et al., 1997) and resolved by polar TLC. Corresponding bands were isolated and lipids were recovered from silica gel by extraction with chloroform-methanol (1:1 by volume). For each PGD1 reaction, 75 nmol lipid substrates extracted from *C. reinhardtii*, or *E. coli* cells expressing the cucumber MGDG synthase were used. The organic solvent was removed under an N_2 stream, and the lipids were resuspended in 350 μL 0.1 M PBS, pH 7.4, with 4.28 mM Triton X-100 and dispersed by sonication (Sonicator 3000 with microprobe; Misonix) for 6 × 10 s (power setting 1.5) on ice. Then, 100 μL additional PBS was added. Per assay, 10 μg refolded PGD1 protein (quantified as stated above) in 50 μL protein refolding buffer was added. As a negative control, 50 μL protein refolding buffer only was added. The PGD1 refolding buffer inhibited *Rhizopus arrhizus* lipase (Sigma-Aldrich). Therefore, 10 μg lipase dissolved in 50 μL PBS instead of protein refolding buffer was used unless otherwise indicated. DTT was added to a final concentration of 1 mM from a freshly prepared stock solution. The mixture was sonicated again for 5 s and incubated at ambient temperature (~22°C). After 6 h incubation (3 h for *R. arrhizus* lipase to prevent potential loss of lyso-lipid standards), reactions were stopped by the addition of 1 mL solvent used for lipid extraction, and lipid extracts were analyzed by TLC described above. For gas chromatograms on free fatty acids and lyso-MGDG generated by PGD1, 9 h was used to obtain more prominent signals. To measure the velocity of MGDG hydrolysis, reactions were quenched after 3 h of incubation.

Positional Analysis of TAG

Positional analysis of TAG was performed with *R. arrhizus* lipase using a similar procedure as described above. Briefly, lipids were extracted from 48 h N-deprived *C. reinhardtii* cells and resolved by neutral TLC. TAG was extracted from silica gel with chloroform-methanol (1:1 by volume) as above. Approximately 10 μg was dried under an N_2 stream and resuspended in PBS containing Triton X-100 as above. *R. arrhizus* lipase was dissolved in PBS, and 20 μg was added to the emulsified TAG preparation. Lipids were extracted from the reaction mixtures and resolved by neutral lipid TLC (described above). Free fatty acids and monoacylglycerol spots were scraped for transesterification as above. Background levels of fatty acids carried over with *R. arrhizus* lipase were estimated in a control reaction without substrate lipid supplied and subtracted from the free fatty acids data obtained with substrate.

Chlorophyll, Viability, and TBARS Analyses

Chlorophylls were extracted from fresh cell pellets with 80% acetone, and concentrations were calculated from the absorbance values at 647 and 664 nm according to Zieger and Egle (1965). To assess cell viability, cells were grown in liquid cultures of TAP or TAP-N. On days 0, 2, 4, and 7, a set volume of culture was diluted and spread onto agar-solidified TAP medium supplemented with 0.4% yeast extract. Colony-forming units were counted 1 week later. Cells from a second aliquot were fixed in 3.7% formaldehyde (in water) and counted using a hemocytometer under a microscope. Viability percentages (colonies formed per total cells counted each day) were normalized to the values on day 0. TBARS were prepared by extraction with thiobarbituric acid/trichloroacetic acid solution (0.3 and 3.9% respectively) and determined by measuring absorbance at 532 nm as previously described (Baroli et al., 2003). The extinction coefficient used was 155 $mM^{-1}cm^{-1}$.

Accession Numbers

Sequence data from this article can be found in the Chlamydomonas v5.3 genome in the Phytozome database, http://www.phytozome.net/, under the following accession numbers: Cre03.g193500 (*PGD1*) and g6364 (*RACK1*).

Supplemental Data

The following materials are available in the online version of this article.

Supplemental Figure 1. Growth Curves of Wild-Type Parental Strain and *pgd1* in Standard TAP Medium.

Supplemental Figure 2. Fatty Acid Compositions of DGTS, PtdEtn, MGDG, DGDG, and PtdGro of the Wild-Type Parental Strain and *pgd1* Mutant in N-Replete Medium and 48 h after Transfer to N-Depleted Medium.

Supplemental Figure 3. In Vivo Pulse-Chase Acetate Labeling of Lipids in the Wild-Type Parental Strain and the *pgd1* Mutant before N Deprivation.

Supplemental Figure 4. In Vivo Pulse-Chase Acetate Labeling of PtdEtn, PtdGro, SQDG, and PtdIns in the Wild-Type Parental Strain and the *pgd1* Mutant.

Supplemental Figure 5. Hydrolysis of *C. reinhardtii*–Derived MGDG by PGD1.

Supplemental Figure 6. Quantitative Hydrolysis of *E. coli*–Derived MGDG by PGD1.

Supplemental Figure 7. Activity of the Recombinant PGD1 Protein on DGTS, PtdEtn, PtdGro, and SQDG.

Supplemental Table 1. Oligonucleotide Primers Used in This Study.

ACKNOWLEDGMENTS

We thank Krishna K. Niyogi and Rachel M. Dent for providing the protocol for SiteFinding PCR and John B. Ohlrogge and Henrik Tjellström

for constructive suggestions on pulse-chase labeling. This research was supported in part by a grant to C.B. from the U.S. Air Force Office of Scientific Research (FA9550-11-1-0264). X.L. was supported in part by a fellowship from the Gene Expression in Development and Disease Focus Group at Michigan State University.

AUTHOR CONTRIBUTIONS

C.B., B.B.S., and M.-H.K. designed the research. X.L., E.R.M., B.L., C.J., M.F., and B.B.S. performed experiments. X.L. and C.B. wrote the article.

Received September 12, 2012; revised October 16, 2012; accepted October 27, 2012; published November 16, 2012.

REFERENCES

Aslanidis, C., and de Jong, P.J. (1990). Ligation-independent cloning of PCR products (LIC-PCR). Nucleic Acids Res. **18:** 6069–6074.

Baroli, I., Do, A.D., Yamane, T., and Niyogi, K.K. (2003). Zeaxanthin accumulation in the absence of a functional xanthophyll cycle protects *Chlamydomonas reinhardtii* from photooxidative stress. Plant Cell **15:** 992–1008.

Baroli, I., Gutman, B.L., Ledford, H.K., Shin, J.W., Chin, B.L., Havaux, M., and Niyogi, K.K. (2004). Photo-oxidative stress in a xanthophyll-deficient mutant of Chlamydomonas. J. Biol. Chem. **279:** 6337–6344.

Bates, P.D., Durrett, T.P., Ohlrogge, J.B., and Pollard, M. (2009). Analysis of acyl fluxes through multiple pathways of triacylglycerol synthesis in developing soybean embryos. Plant Physiol. **150:** 55–72.

Bates, P.D., Ohlrogge, J.B., and Pollard, M. (2007). Incorporation of newly synthesized fatty acids into cytosolic glycerolipids in pea leaves occurs via acyl editing. J. Biol. Chem. **282:** 31206–31216.

Benning, C. (2009). Mechanisms of lipid transport involved in organelle biogenesis in plant cells. Annu. Rev. Cell Dev. Biol. **25:** 71–91.

Benning, C., Huang, Z.H., and Gage, D.A. (1995). Accumulation of a novel glycolipid and a betaine lipid in cells of *Rhodobacter sphaeroides* grown under phosphate limitation. Arch. Biochem. Biophys. **317:** 103–111.

Berthold, P., Schmitt, R., and Mages, W. (2002). An engineered *Streptomyces hygroscopicus* aph 7′′ gene mediates dominant resistance against hygromycin B in *Chlamydomonas reinhardtii*. Protist **153:** 401–412.

Browse, J., Warwick, N., Somerville, C.R., and Slack, C.R. (1986). Fluxes through the prokaryotic and eukaryotic pathways of lipid synthesis in the '16:3' plant *Arabidopsis thaliana*. Biochem. J. **235:** 25–31.

Castruita, M., Casero, D., Karpowicz, S.J., Kropat, J., Vieler, A., Hsieh, S.I., Yan, W.H., Cokus, S., Loo, J.A., Benning, C., Pellegrini, M., and Merchant, S.S. (2011). Systems biology approach in *Chlamydomonas* reveals connections between copper nutrition and multiple metabolic steps. Plant Cell **23:** 1273–1292.

Chang, C.W., Moseley, J.L., Wykoff, D., and Grossman, A.R. (2005). The LPB1 gene is important for acclimation of *Chlamydomonas reinhardtii* to phosphorus and sulfur deprivation. Plant Physiol. **138:** 319–329.

Chen, H.H., Wickrema, A., and Jaworski, J.G. (1988). Acyl-acyl-carrier protein: Lysomonogalactosyldiacylglycerol acyltransferase from the cyanobacterium *Anabaena variabilis*. Biochim. Biophys. Acta **963:** 493–500.

Chen, W., Sommerfeld, M., and Hu, Q.A. (2011). Microwave-assisted nile red method for in vivo quantification of neutral lipids in microalgae. Bioresour. Technol. **102:** 135–141.

Davies, J.P., Yildiz, F.H., and Grossman, A. (1996). Sac1, a putative regulator that is critical for survival of *Chlamydomonas reinhardtii* during sulfur deprivation. EMBO J. **15:** 2150–2159.

Draber, W., Trebst, A., and Harth, E. (1970). On a new inhibitor of photosynthetic electron-transport in isolated chloroplasts. Z. Naturforsch. B **25:** 1157–1159.

Durrett, T.P., Benning, C., and Ohlrogge, J. (2008). Plant triacylglycerols as feedstocks for the production of biofuels. Plant J. **54:** 593–607.

Fan, J., Yan, C., Andre, C., Shanklin, J., Schwender, J., and Xu, C. (2012). Oil accumulation is controlled by carbon precursor supply for fatty acid synthesis in *Chlamydomonas reinhardtii*. Plant Cell Physiol. **53:** 1380–1390.

Fan, J.L., Andre, C., and Xu, C.C. (2011). A chloroplast pathway for the de novo biosynthesis of triacylglycerol in *Chlamydomonas reinhardtii*. FEBS Lett. **585:** 1985–1991.

Fernández, E., Schnell, R., Ranum, L.P.W., Hussey, S.C., Silflow, C.D., and Lefebvre, P.A. (1989). Isolation and characterization of the nitrate reductase structural gene of *Chlamydomonas reinhardtii*. Proc. Natl. Acad. Sci. USA **86:** 6449–6453.

Fischer, B.B., Krieger-Liszkay, A., Hideg, E., Snyrychová, I., Wiesendanger, M., and Eggen, R.I. (2007). Role of singlet oxygen in chloroplast to nucleus retrograde signaling in *Chlamydomonas reinhardtii*. FEBS Lett. **581:** 5555–5560.

Fischer, W., Heinz, E., and Zeus, M. (1973). The suitability of lipase from *Rhizopus arrhizus delemar* for analysis of fatty acid distribution in dihexosyl diglycerides, phospholipids and plant sulfolipids. Hoppe Seylers Z. Physiol. Chem. **354:** 1115–1123.

Giroud, C., and Eichenberger, W. (1989). Lipids of *Chlamydomonas reinhardtii* - Incorporation of [C-14] acetate, [C-14] palmitate and [C-14] oleate into different lipids and evidence for lipid-linked desaturation of fatty acids. Plant Cell Physiol. **30:** 121–128.

Giroud, C., Gerber, A., and Eichenberger, W. (1988). Lipids of *Chlamydomonas reinhardtii* - Analysis of molecular species and intracellular site(s) of biosynthesis. Plant Cell Physiol. **29:** 587–595.

Goodson, C., Roth, R., Wang, Z.T., and Goodenough, U. (2011). Structural correlates of cytoplasmic and chloroplast lipid body synthesis in *Chlamydomonas reinhardtii* and stimulation of lipid body production with acetate boost. Eukaryot. Cell **10:** 1592–1606.

Grossman, A.R., Harris, E.E., Hauser, C., Lefebvre, P.A., Martinez, D., Rokhsar, D., Shrager, J., Silflow, C.D., Stern, D., Vallon, O., and Zhang, Z.D. (2003). *Chlamydomonas reinhardtii* at the crossroads of genomics. Eukaryot. Cell **2:** 1137–1150.

Harris, E.H. (1989). Chlamydomonas Sourcebook. (New York: Academic Press).

Heinz, E., and Roughan, P.G. (1983). Similarities and differences in lipid metabolism of chloroplasts isolated from 18:3 and 16:3 plants. Plant Physiol. **72:** 273–279.

Hu, Q., Sommerfeld, M., Jarvis, E., Ghirardi, M., Posewitz, M., Seibert, M., and Darzins, A. (2008). Microalgal triacylglycerols as feedstocks for biofuel production: Perspectives and advances. Plant J. **54:** 621–639.

James, G.O., Hocart, C.H., Hillier, W., Chen, H.C., Kordbacheh, F., Price, G.D., and Djordjevic, M.A. (2011). Fatty acid profiling of *Chlamydomonas reinhardtii* under nitrogen deprivation. Bioresour. Technol. **102:** 3343–3351.

Joyard, J., Block, M.A., and Douce, R. (1991). Molecular aspects of plastid envelope biochemistry. Eur. J. Biochem. **199:** 489–509.

Kimura, K., Yamaoka, M., and Kamisaka, Y. (2004). Rapid estimation of lipids in oleaginous fungi and yeasts using Nile red fluorescence. J. Microbiol. Methods **56:** 331–338.

Kindle, K.L. (1990). High-frequency nuclear transformation of *Chlamydomonas reinhardtii*. Proc. Natl. Acad. Sci. USA **87:** 1228–1232.

Kunst, L., Browse, J., and Somerville, C. (1988). Altered regulation of lipid biosynthesis in a mutant of *Arabidopsis* deficient in chloroplast

glycerol-3-phosphate acyltransferase activity. Proc. Natl. Acad. Sci. USA **85:** 4143–4147.

Li, X., Benning, C., and Kuo, M.H. (October 5, 2012). Rapid triacylglycerol turnover in *Chlamydomonas reinhardtii* requires a lipase with broad substrate specificity. Eukaryot. Cell. (online), doi: 10.1128/EC.00268-12.

Liu, B. and Benning, C. (September 12, 2012). Lipid metabolism in microalgae distinguishes itself. Curr. Opin. Biotechnol. (online), doi: pii: S0958-1669(12)00122-X. 10.1016/j.copbio.2012.08.008.

Livak, K.J., and Schmittgen, T.D. (2001). Analysis of relative gene expression data using real-time quantitative PCR and the 2(-Delta Delta C(T)) Method. Methods **25:** 402–408.

Lu, B., and Benning, C. (2009). A 25-amino acid sequence of the *Arabidopsis* TGD2 protein is sufficient for specific binding of phosphatidic acid. J. Biol. Chem. **284:** 17420–17427.

Lu, Y., Savage, L.J., Ajjawi, I., Imre, K.M., Yoder, D.W., Benning, C., Dellapenna, D., Ohlrogge, J.B., Osteryoung, K.W., Weber, A.P., Wilkerson, C.G., and Last, R.L. (2008). New connections across pathways and cellular processes: industrialized mutant screening reveals novel associations between diverse phenotypes in *Arabidopsis*. Plant Physiol. **146:** 1482–1500.

Luo, J., Xu, X., Hall, H., Hyland, E.M., Boeke, J.D., Hazbun, T., and Kuo, M.H. (2010). Histone h3 exerts a key function in mitotic checkpoint control. Mol. Cell. Biol. **30:** 537–549.

Ma, H., Kunes, S., Schatz, P.J., and Botstein, D. (1987). Plasmid construction by homologous recombination in yeast. Gene **58:** 201–216.

Mehler, A.H. (1951). Studies on reactions of illuminated chloroplasts. II. Stimulation and inhibition of the reaction with molecular oxygen. Arch. Biochem. Biophys. **34:** 339–351.

Merchant, S.S., et al. (2007). The Chlamydomonas genome reveals the evolution of key animal and plant functions. Science **318:** 245–250.

Miller, R., et al. (2010). Changes in transcript abundance in *Chlamydomonas reinhardtii* following nitrogen deprivation predict diversion of metabolism. Plant Physiol. **154:** 1737–1752.

Moellering, E.R., and Benning, C. (2010). RNA interference silencing of a major lipid droplet protein affects lipid droplet size in *Chlamydomonas reinhardtii*. Eukaryot. Cell **9:** 97–106.

Moellering, E.R., Muthan, B., and Benning, C. (2010). Freezing tolerance in plants requires lipid remodeling at the outer chloroplast membrane. Science **330:** 226–228.

Newman, S.M., Boynton, J.E., Gillham, N.W., Randolph-Anderson, B.L., Johnson, A.M., and Harris, E.H. (1990). Transformation of chloroplast ribosomal RNA genes in *Chlamydomonas*: Molecular and genetic characterization of integration events. Genetics **126:** 875–888.

Nguyen, H.T., Mishra, G., Whittle, E., Pidkowich, M.S., Bevan, S.A., Merlo, A.O., Walsh, T.A., and Shanklin, J. (2010). Metabolic engineering of seeds can achieve levels of omega-7 fatty acids comparable with the highest levels found in natural plant sources. Plant Physiol. **154:** 1897–1904. Erratum. Plant Physiol. **155:** 1473.

Ohlrogge, J.B., Kuhn, D.N., and Stumpf, P.K. (1979). Subcellular localization of acyl carrier protein in leaf protoplasts of *Spinacia oleracea*. Proc. Natl. Acad. Sci. USA **76:** 1194–1198.

Riekhof, W.R., Sears, B.B., and Benning, C. (2005). Annotation of genes involved in glycerolipid biosynthesis in *Chlamydomonas reinhardtii*: Discovery of the betaine lipid synthase BTA1Cr. Eukaryot. Cell **4:** 242–252.

Robert, G., Melchiorre, M., Trippi, V., and Lascano, H.R. (2009). Apoplastic superoxide level in wheat protoplast under photooxidative stress is regulated by chloroplast ROS generation: Effects on the antioxidant system. Plant Sci. **177:** 168–174.

Rossak, M., Schäfer, A., Xu, N., Gage, D.A., and Benning, C. (1997). Accumulation of sulfoquinovosyl-1-O-dihydroxyacetone in a sulfolipid-deficient mutant of *Rhodobacter sphaeroides* inactivated in *sqdC.* Arch. Biochem. Biophys. **340:** 219–230.

Roughan, P.G., and Slack, C.R. (1982). Cellular organization of glycerolipid metabolism. Annu. Rev. Plant Physiol. Plant Mol. Biol. **33:** 97–132.

Rousseeuw, P.J., and Croux, C. (1993). Alternatives to the median absolute deviation. J. Am. Stat. Assoc. **88:** 1273–1283.

Sato, N., and Murata, N. (1991). Transition of lipid phase in aqueous dispersions of diacylglyceryltrimethylhomoserine. Biochim. Biophys. Acta **1082:** 108–111.

Shimojima, M., Ohta, H., Iwamatsu, A., Masuda, T., Shioi, Y., and Takamiya, K. (1997). Cloning of the gene for monogalactosyldiacylglycerol synthase and its evolutionary origin. Proc. Natl. Acad. Sci. USA **94:** 333–337.

Shulaev, V., and Oliver, D.J. (2006). Metabolic and proteomic markers for oxidative stress. New tools for reactive oxygen species research. Plant Physiol. **141:** 367–372.

Siebertz, H.P., and Heinz, E. (1977). Labelling experiments on the origin of hexa- and octadectrienoic acids in galactolipids from leaves. Z. Naturforsch. C **32c:** 193–205.

Tan, G.H., Gao, Y., Shi, M., Zhang, X.Y., He, S.P., Chen, Z., and An, C.C. (2005). SiteFinding-PCR: A simple and efficient PCR method for chromosome walking. Nucleic Acids Res. **33:** e122.

Wang, Z.T., Ullrich, N., Joo, S., Waffenschmidt, S., and Goodenough, U. (2009). Algal lipid bodies: Stress induction, purification, and biochemical characterization in wild-type and starchless *Chlamydomonas reinhardtii*. Eukaryot. Cell **8:** 1856–1868.

Wen, F., Xing, D., and Zhang, L. (2008). Hydrogen peroxide is involved in high blue light-induced chloroplast avoidance movements in *Arabidopsis*. J. Exp. Bot. **59:** 2891–2901.

Weyer, K.M., Bush, D.R., Darzins, A., and Willson, B.D. (2010). Theoretical maximum algal oil production. Bioenergy Res. **3:** 204–213.

Work, V.H., Radakovits, R., Jinkerson, R.E., Meuser, J.E., Elliott, L.G., Vinyard, D.J., Laurens, L.M.L., Dismukes, G.C., and Posewitz, M.C. (2010). Increased lipid accumulation in the *Chlamydomonas reinhardtii* sta7-10 starchless isoamylase mutant and increased carbohydrate synthesis in complemented strains. Eukaryot. Cell **9:** 1251–1261.

Xu, C., Fan, J., Riekhof, W., Froehlich, J.E., and Benning, C. (2003). A permease-like protein involved in ER to thylakoid lipid transfer in *Arabidopsis*. EMBO J. **22:** 2370–2379.

Zieger, R., and Egle, K. (1965). Zur quantitativen Analyse der Chloroplasten pigmente. I. Kritische Überprüfung der spektralphotometrischen Chlorophyllbestimmung. Beitr. Biol. Pflanz. **41:** 11–37.